FACULTY OF TECHNOLOGY

EFFECT OF WATER ON CELLULOSE TREATMENT WITH CHOLINE CHLORIDE -UREA DEEP EUTECTIC SOLVENT

Riikka Haataja

ENVIRONMENTAL ENGINEERING

Master's thesis

November 2021

ABSTRACT

Effect of water on cellulose treatment with choline chloride-urea deep eutectic solvent

Riikka Haataja

University of Oulu, Environmental Engineering

Master's thesis 2021, 78 pp. 3 appendixes

Supervisors at the university: Juho Sirviö, Terhi Suopajärvi, Henrikki Liimatainen

Deep eutectic solvents (DES) have emerged as a new green solvent class which have many advantages over conventional solvents. One of the numerous applications for DESs is treatment of cellulose fibers. The aim of this study was to find out if aqueous solutions of choline chloride and urea (CC:U) could be used to swell cellulose fibers and how water affects the properties of CC:U. In addition, various methods to determine Kamlet-Taft polarity parameters for aqueous CC:U were explored as they have not yet been determined in literature.

Cellulose pulp was treated with 18 CC:U DESs with different molar ratios and water contents. The fiber properties were measured to observe possible swelling and cellulose hydrolysis. Fourier transform infrared spectroscopy (FTIR) was used to perceive if chemical reactions had occurred during the DES treatment. The reactivity of DES pretreated cellulose was studied with conductometric titration after (2,2,6,6-tetramethyl-piperidin-1-yl)oxyl (TEMPO) treatment. Moreover, DES properties such as viscosity, conductivity, and pH were examined. Kamlet-Taft polarity parameters were determined with solvatochromic and solvatomagnetic methods.

It was found that treatment efficiency of CC:U did not decrease remarkably with increasing water content. However, the largest fiber widths were obtained with treatments without mixing. FTIR measurements indicated that no chemical reactions had occurred during the cellulose treatment. DES pH decreased and conductivity increased with increasing water content while viscosity decreased with increasing temperature and shear rate. Most reasonable Kamlet-Taft parameter values were obtained with combination of solvatochromic and solvatomagnetic methods. Kamlet-Taft parameters could also be used

to evaluate the swelling properties of solvent. As a result of the study, it can be concluded that water does dot degrade swelling efficiency and eases the handling of CC:U.

Keywords: DES, cellulose, fiber swelling

TIIVISTELMÄ

Veden vaikutus selluloosan käsittelyyn koliinikloridi-urea syväeutektisella liuottimella

Riikka Haataja

Oulun Yliopisto, Ympäristötekniikka

Diplomityö 2021, 82 s. 3 liitettä

Työn ohjaajat yliopistolla: Juho Sirviö, Terhi Suopajärvi, Henrikki Liimatainen

Syväeutektiset liuottimet (Deep eutectic solvents, DES) ovat herättäneet kiinnostusta uudentyyppisinä vihreinä liuottimina, sillä niillä on monia etuja verrattuna perinteisiin liuottimiin. Yksi lukuisista DES:ien sovellutuksista on selluloosakuitujen turvottaminen. Tämän työn tarkoituksena oli selvittää, voidaanko vesipitoista koliikloridi-ureaa (choline chloride:urea, CC:U) käyttää selluloosakuitujen turvottamiseen ja millä tavoin vesi vaikuttaa CC:U:n rakenteeseen. Lisäksi tutkittiin useita eri menetelmiä Kamlet-Taft-polaarisuusparametrien määrittämiseksi vesipitoisille CC:U:lle, sillä niitä ei ole vielä esitetty kirjallisuudessa.

Selluloosamassaa käsiteltiin 18:sta eri CC:U DES:llä, joilla oli toisistaan poikkeavat moolisuhteet ja vesipitoisuudet. Kuitujen morfologisia ominaisuuksia tutkittiin turpoamisen ja pilkkoutumisen havaitsemiseksi ja mahdollisia käsittelyn aikana tapahtuneita kemiallisia muutoksia havainnoitiin Fourier-infrapunaspektroskopialla. DES-käsitelty sellu hapetettiin (2,2,6,6-tetramethyl-piperidin-1-yl)oxyl (TEMPO)-reagenssilla, jonka jälkeen sellun reaktiivisuus määritettiin konduktometrisellä titrauksella. DES:ien ominaisuuksista määritettiin viskositeetti, pH ja johtokyky. Lisäksi määritettiin DES:ien Kamlet-Taft-parametrit solvatokromisella ja solvatomagnettisella menetelmällä.

Tutkimuksessa havaittiin, että CC:U käsittelyn tehokkuus ei merkittävästi heikentynyt vesipitoisuuden kasvaessa. Suurin kuitujen turpoaminen saatiin aikaan käsittelemällä sellu ilman sekoitusta. Fourier-infrapunaspektroskopia osoitti, että kemiallisia muutoksia ei ollut tapahtunut DES-käsittelyjen aikana. Liuottimien pH laski ja johtokyky nousi vesipitoisuuden kasvaessa, kun taas viskositeetin havaittiin laskevan lämpötilan ja leikkausvoiman kasvaessa. Luotettavimmat Kamlet-Taft-parametrit saatiin

solvatokromisen ja solvatomagnettisen menetelmän yhdistelmällä. Tutkimuksessa havaittiin myös, että näitä parametrejä voidaan käyttää arvioimaan liuottimen kykyä turvottaa selluloosakuituja. Tämän työn lopputuloksena voidaan todeta, että vesi ei huononna CC:U:n tehoa, mutta helpottaa sen käsittelyä.

Asiasanat: DES, selluloosa, kuitujen turvottaminen

FOREWORD

In this study the efficiency of aqueous choline chloride:urea DESs in cellulose swelling was investigated. The effect of water on DES properties was also explored. This work was done at Fibre and Particle Engineering Research Unit of University of Oulu in a time period of six months. I want to thank my supervisors Juho Sirviö, Terhi Suopajärvi and Henrikki Liimatainen for their guidance and discussions on this project. Also, I want to thank Anu Kantola for help and advice on NMR measurements. Special thanks to Jani Österlund, Elisa Wirkkala and Jarno Karvonen who are always ready to help at laboratory work.

Oulu, 3.11.2021

Riikka Haataja
Riikka Haataja

TABLE OF CONTENTS

ABSTRACT 1
TIIVISTELMÄ 3
FOREWORD 5
TABLE OF CONTENTS 6
LIST OF ABBREVIATIONS 8
1 INTRODUCTION 9
2 CELLULOSE 11
2.1 Molecular structure 11
2.2 Applications 13
3 DEEP EUTECTIC SOLVENTS 14
3.1 DES structure and properties 14
3.2 DES toxicity and biodegradability 16
3.3 Aqueous choline chloride:urea 17
3.4 DES polarity 19
3.4.1 Solvatochromic method 19
3.4.2 Solvatomagnetic method 23
3.5 DES and cellulose 24
4 EXPERIMENTAL 26
4.1 Cellulose treatment 26
4.1.1 Cellulose treatment without mixing 28
4.2 Fiber analysis 28
4.2.1 Fiber properties 28
4.2.2 Diffuse reflectance infrared Fourier transform spectroscopy 28
4.2.3 Cellulose reactivity 29
4.2.4 Nanofibrillation 32
4.3 DES properties 32
4.3.1 Viscosity, pH and conductivity 33
4.3.2 Solvatochromic method 34
4.3.3 Solvatomagnetic method 35
5 RESULTS AND DISCUSSION 37
5.1 Cellulose treatment 37
5.1.1 Fiber properties of DES pretreated cellulose 37
5.1.2 The influence of mixing on DES pretreatment 42

5.1.3 FTIR 44
5.1.4 Determination of acidic groups 50
5.1.5 Nanofibrillation 51
5.2 DES properties 51
5.2.1 Viscosity 51
5.2.2 pH 54
5.2.3 Conductivity 56
5.2.4 Kamlet-Taft parameters 58
5.2.5 Relationship of polarity parameters and fiber swelling 67
6 SUMMARY 69
REFERENCES 71
APPENDICES:
Appendix 1. FS5 analysis, all particles.
Appendix 2. Wavelengths corresponding to maximum absorption of the probes 4-nitroaniline (4NA), N,N-diethyl-4-nitroaniline (DENA) and Nile Red (NR).
Appendix 3. Viscosities of DESs with different shear rates in 20 °C and in 100 °C.

LIST OF ABBREVIATIONS

4NA	4-nitroaniline
CC	choline chloride
CNC	cellulose nanocrystals
CNF	cellulose nanofibers
CC:U	choline chloride-urea DES
DES	deep eutectic solvent
DENA	N,N-diethyl-4-nitroaniline
DMSO	diethyl sulfoxide
DP	degree of polymerization
DRIFT	diffuse reflectance Fourier transform spectroscopy
FTIR	Fourier-transform infrared spectroscopy
HBA	hydrogen bond acceptor
HBD	hydrogen bond donor
LSER	linear solvation energy relationship
NR	Nile red

α	Kamlet-Taft hydrogen bond acidity
β	Kamlet-Taft hydrogen bond basicity
π^*	Kamlet-Taft dipolarity/dipolarizability

1 INTRODUCTION

Solvents have often an important role in applications of chemical industry. Following the principles of sustainable chemistry, more safe and environmentally friendly alternatives are needed for conventional solvents. (Alonso et al. 2016) Deep eutectic solvents (DES) are new generation of greener solvents which have many advantages over their predecessors. DESs have a lower melting point than their individual components and can be easily produced by mixing together the components (Abbott et al. 2004). DESs are generally readily biodegradable (Juneidi et al. 2015, Lapena et al. 2021), less toxic than conventional solvents (Hayyan et al. 2015, Jung et al. 2021), and their components are relatively low-cost (Sirviö et al. 2015, Tome et al. 2018). DESs can be easily produced by combining hydrogen bond donor (HBD) and hydrogen bond acceptors (HBA). Wide scale of HBA and HBD components allows DESs to be customized to various applications (Hayyan et al. 2013, Singh et al. 2011, Chen et al. 2019, Ma et al. 2019).

Cellulose is the most abundant biopolymer in the world. Novel applications of cellulose have emerged with increasing research on its structure and properties. (Heinze et al. 2016) One of the most remarkable new applications are nanocellulose materials, which have unique properties giving it potential to be used to replace fossil-based materials. Nanocellulose materials can be produced from cellulose with mechanical treatment which is however rather energy-intensive process. (Klemm et al. 2011) Energy demand can be decreased with chemical pretreatment in which various DESs have been used. Prereatment of cellulose with DES loosens the structure of cellulose hydrogen bond network without hydrolysing the fibers. (Sirviö et al. 2015, Tenhunen et al. 2018) As a result, fibers swell which can be observed as increased fiber width (Sirviö et al. 2015). The DES swollen fibers can further be harnessed in nanocellulose production, cellulose dissolution and derivatization, for example.

Swelling of the fibers has so far been studied mainly with pure DESs in the absence of water (Li et al. 2017, Sirviö et al. 2015, Tenhunen et al. 2018, Zhang et al 2020). However, cellulose and many DESs such as CC:U and its components are strongly hygroscopic, and it would be highly practical to use aqueous DES in the cellulose treatment to avoid drying processes and lower the high viscosity of DESs (Abbott et al. 2004). The aim of this study was to investigate aqueous DES of CC:U in swelling of cellulose pulp fibers and to find optimal molar ratio of CC:U. The effect of water and different molar ratios on

CC:U viscosity, pH and conductivity was also examined. So far there has not been any research on Kamlet-Taft parameters of aqueous CC:U. Several methods to determine these parameters were evaluated in this study.

2 CELLULOSE

Currently, there is a high demand for finding sustainable materials for replacing fossil-based products. At the moment, cellulose use as a sustainable alternative is mainly restricted due to its insolubility in water, hygroscopicity, and absence of thermoformability. (Nechyporchuk et al. 2016) Cellulose can be modified to nanocellulose materials with unique properties enabling novel applications (Klemm et al. 2018), such as environmentally friendly cellulose aerogels (Chen et al. 2021) and cellulose packaging materials to replace oil-based plastics (Fotie et al. 2020).

Cellulose is the most abundant natural polymer which makes it an interesting component for various industrial applications. Other advantageous properties of cellulose are nontoxicity, biodegradability and renewability. Also, cellulose is non-edible which makes it ethically more acceptable raw material compared to many other materials such as starch based materials. Cellulose can be found for example in wood and other plants or agricultural waste. About 40% of wood is cellulose and in plants it is often accompanied with lignin, hemicellulose and extractives. (Heinze et al. 2016)

The chemical properties and reactivities of cellulose molecules are determined by inter- and intramolecular interactions, cross-linking reactions, polymer chain lengths, distribution of polymer chains and distribution of functional groups on the repeating units. Cellulose exhibits higher chain stiffness, distinct polyfunctionality, and is more sensitive to hydrolysis and oxidation of chain forming acetal groups than synthetic polymers. (Klemm et al. 2005)

2.1 Molecular structure

Cellulose is a macromolecule which consists of repeating anhydroglucose (AGU) units. The degree of polymerization (DP) describes the number of individual AGUs in the cellulose chain. The DP value depends on the cellulose source and it is typically 300-1700 with wood pulp. The molecular structure causes cellulose to be hydrophilic, chiral and degradable. The high reactivity of OH-groups initiates the wide chemical variability of cellulose. (Klemm et al. 2005) Chemical cellulose pulps contain usually more carbonyl groups than non-treated cellulose due to oxidative treatment. (Röhrling et al. 2002)

In cellulose polymer β-D-glucopyranose molecules are covalently linked by equatorial OH-groups of C4 and C1 resulting in a linear polymer with large number of hydroxyl groups. Every second AGU ring is rotated 180 ° to accommodate the preferred bond angles of the acetal oxygen bridges. The non-reducing end of cellulose chain consists of original C4-OH group at the one end of D-glucose unit and the reducing end is terminated with original C1-OH which is in equilibrium with aldehyde structure. The hydroxyl groups are placed in C2, C3 and C6. The CH_2OH side group is in a trans-gauche position relating to O5-C5 and C4-C5 bonds. (Klemm et al. 2005) The molecular structure of cellulose is presented in Figure 1.

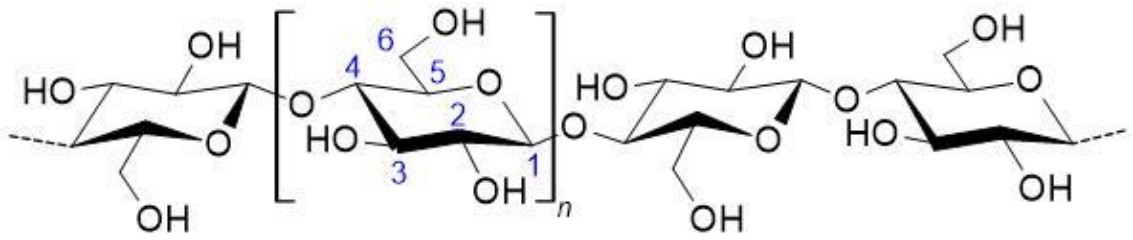

Figure 1. Cellulose molecular structure.

Cellulose chain contains non-covalent bonds resulting in supramolecular structure with both less-ordered (amorphous) and crystalline areas. (Klemm et al. 2005) Hydrogen bonds also strongly determine other properties, such as poor solubility and resistance of cellulose to swelling. Especially free primary OH group at C6 position favorably forms intermolecular bonds, their number is important to cellulose solubility. It is also noted that cellulose derivatives with blocked C6 OH groups show almost no crystallinity at all. (Kondo et al. 1997)

Cellulose molecular structure can change due to chemical reactions which hydrolyze or oxidate the cellulose chain. These reactions mainly take place on the fibril surfaces or in the amorphous regions. (Heinze et al. 2016) Reactivity of cellulose molecule is decreased if OH groups are bonded in the reaction medium with hydrogen bonds. Especially OH groups in C2 are considered to be highly reactive but if it is occupied with an intramolecular hydrogen bond to ether oxygen of a methoxy group at C6, the relative reactivity is notably lower. (Kondo et al. 1997)

2.2 Applications

Increased knowledge about structure and reactivity has led to continuous creation of novel cellulose applications and products, such as pharmaceuticals, films, coatings and filaments. (Klemm et al. 2011) Current interest is especially on cellulose-based biocomposites, hybrid materials and nanocellulose applications. (Hiba et al. 2018) Non-treated cellulose has a limited innate activity for beneficiation, but chemical modifications of its three hydroxyl groups (Selkälä et al. 2016) allow the attachment of desired functional components on the cellulose structure. (Sirviö et al. 2015)

Cellulose can be further processed to individualized nanocellulose particles which have at least one dimension in 1-100 nm scale (Nechyporchuk et al. 2016) which have unique properties compared to native cellulose (Klemm et al. 2011). Nanocelluloses can be divided to two main classes, cellulose nanocrystals (CNC) and cellulose nanofibers (CNF) (Nechyporchuk et al. 2016), but their nomenclature is not explicitly established. (Klemm et al. 2011). CNC consists of rodlike cellulose crystals with varying widths and lengths. It is produced by acid hydrolysis of cellulose from various sources. CNF consists of roughly 4-20 nm wide fibrils which exhibit gel-like properties in water. CNF can be produced by delamination of pulp with mechanical disintegration. (Klemm et al. 2011) However, as the hydrogen bond network of cellulose is highly ordered (Sirviö et al. 2015), mechanical treatments are rather energy-intensive processes. Therefore, new pretreatment methods are studied to optimize the production of nanocellulose (Nechyporchuk et al. 2016). Energy demand can be reduced for example with enzymatic or chemical pretreatments (Bharimalla et al.2015).

3 DEEP EUTECTIC SOLVENTS

Continuous search for green technologies and methods is ongoing to explore more sustainable ways to utilize world's limited resources. Solvents are needed for reaction media and they are consumed in vast amounts. To avoid environmental and economic drawbacks of the conventional solvents, many alternative solvents have been revealed. (Alonso et al. 2016) Ionic liquids have been investigated as a new type of efficient customizable solvents. They are generally liquid in room temperature, easily adaptable, non-flammable, and they do not emit volatile compounds as their vapor pressure in negligible. (Earle & Seddon 2002) However, typically they are not biodegradable (Docherty et al 2007, Gathergood et al. 2004) and they have a toxic nature (Zhao et al. 2007).

Eutectic mixture solvents were first introduced in 2001 by Abbott et al. as a cost-effective and moisture-stable alternative for ionic liquids. Eutectic mixture have a lower melting point than its individual components and they can be easily synthetized from pure state by complexing hydrogen bond acceptors (HBA) and hydrogen bond donors (HBD), for example choline chloride (CC) and urea. (Abbott et al. 2004) Deep eutectic solvent (DES) term was introduced to separate these solvents from ionic liquids (Abbott et al. 2004) and they have aroused growing interest in last decades (Scopus database 2021).

3.1 DES structure and properties

In 2003 Abbott et al. showed that eutectic mixtures of quaternary ammonium salts and amides are formed via hydrogen bonds and they have similar solvent properties to ionic liquids. Strong hydrogen bonds decrease the cation-anion interactions of the HBA which results in a remarkably lower freezing point (Teles et al. 2017). The fluid properties like viscosity of DES depend on the molar ratio of the mixture but they are also linked to the size of the mobile species and the availability of holes of appropriate dimensions to allow mobility. (Abbott et al. 2004)

Compared to conventional solvents or ionic liquids, DESs are non-flammable (Skulcova et al. 2018), relatively low-cost and their components are more readily available (Tome et al. 2018). DESs also have low vapor emissions (Wu et al. 2012) and good recyclability (Hayyan et al. 2013, Singh et al. 2011). These properties make DESs highly promising

solvents to be used in the framework of green chemistry. The variety of HBA and HBD combinations offer the possibility to create customized DESs for different applications, for example catalysing biodiesel production (Hayyan et al. 2013), selective alkylation of amines (Singh et al. 2011), food analysis (Chen et al. 2019), or production of nanocellulose (Ma et al. 2019).

DESs can be described by the general formula Cat^+X^-zY. Cat^+ is a cation of any phosphonium, sulfonium or ammonium salt and X^- is a Lewis base, often halide anion. Y can be either Lewis or Bronsted acid and z indicates the number of Y's. Depending on their complexing agent, DESs can be classified into four main types. Type I DESs consist of metal halide and quaternary ammonium salts, such as chloroaluminate and imidazolium salt melts. Choline is a commonly used as Cat^+ due to its relatively low-cost and low toxicity. Nonhydrated halides with suitably low melting point are, however, thin on the ground and have often relatively high costs. Type II DESs expand the scale by using hydrated metal halides as Y, which makes these solvent generally lower cost. Type III DESs consist of hydrogen bond donors, such as amides and carboxylic acids, complexed with quaternary ammonium salts. The wide range of hydrogen bond donors makes DESs of this type especially adaptable. Type IV DESs are mixtures of certain metal halides and hydrogen bond donors, such as $ZnCl_2$ and acetamide. (Smith et al. 2014) Lately, Abranches et al. (2019) showed that DES can be formed from thymol and menthol, which are both non-ionic molecular components. Non-ionic DESs can be classified as type V DESs (Abranches et al. 2019, Mannu et al. 2021, Schaeffer et al. 2021)

Conductivity, viscosity and pH

Solvent pH has an important role in the chemical reactions, especially catalysis, biochemical reactions or metal treatment. In biomass fractionation processes non-suitable pH may lead to losing valueble biomass properties by unwanted reactions (Skulcova et al. 2018) such as hydrolysis of cellulose fibers. (Palme et al. 2018) With increasing HBD content, the pH values of various DESs typically decreases. Increase of temperature also decreases pH. (Skulcova et al. 2018)

Conductivity of DESs is high compared to traditional molecular solvents which allows DESs to be utilized in electrochemical applications. (Abbott et al. 2006) However, DESs have also often high viscosity which has a concomitant effect on conductivity: because

the fluidity of the mixture is mainly limited by size and availability holes in the solution structure, the viscosity limits the ionic mobility. (Abbott et al. 2004) High viscosity causes deteriorated flow, decreased mass transfer of solutes (Gajardo-Parra et al. 2020) and thus can lead to difficulties in extraction, removal, transportation and recycling (Skulcova et al. 2018) which can prevent successful industrial applications. Increasing the process temperature lowers the viscosity, (Gajardo-Parra et al. 2020) but as the higher reaction temperature increases energy consumption, environmentally better option would be to alter the viscosity. Viscosity can be decreased by tailoring a DES from smaller HBA and HBD molecules (Abbott et al. 2006) but also by introducing water to DES mixture (Du et al. 2016, Gygli et al. 2020, Xie et al. 2014). Using aqueous DESs would be economically and environmentally better way to enhance the DES performance if the effect of water does not impair the process remarkably.

3.2 DES toxicity and biodegradability

DESs are often referred as nontoxic solvents based on the properties of the separate components (Abbott et al. 2004, Mannu et al. 2021, Singh et al. 2012, Zhang et al. 2012). However, Hayyan et al. (2013) investigated toxicity and cytotoxicity of various DESs on bacteria and noted that all tested DESs had higher cytotoxicity than their components. Jung et al. (2021) noted in their metabolomic analysis of CC:U DES on mice that DES solutions were often more cytotoxic than their individual components but aqueous solutions of DESs were noted to be less harmful than pure solvents. Causes for the toxic effects on metabolisms were suggested to derive from the presence of ammonia in the solvent and from oxidative stress in liver, kidney and serum. (Jung et al. 2021) Toxic properties of DESs are highly dependent on molar ratio and components, which was demonstrated with LD_{50} tests on mice: CC:U DES with molar ratio of 1:3 caused an immediate death on animals, thus the LD_{50}value could not be determined. Instead, same DES with molar ratio 1:2 showed LD_{50} at 5.64 g/kg. For comparison, both components individually showed LD50 values over 20 g/kg. However, DESs are often less toxic than ionic liquids (Hayyan et al. 2015). General statements about toxicity of DESs should be made with caution and the toxicity properties should be defined for individual DESs before their industrial usage.

Similarly, biodegradability of DESs is often deducted from the properties of individual compounds (Abbott et al. 2001, Zhang et al. 2012). Juneidi et al. (2015) studied the

biodegradability of several DESs according to OECD standard and all of them were shown to be readily biodegradable. However, Wen et al. (2015) tested biodegradability of eight DESs and noted that only two of tested DESs could be defined as readily biodegradable, namely 1:1 CC:U and CC:acetamide. Contradictory results were obtained for some DESs which had been tested in both studies, for example CC:ethylene glycol. Lapena et al. (2021) investigated biodegradability of three pure DESs and their aqueous solvents. All pure DESs were noted to be readily biodegradable but of aqueous DESs only CC:U exhibited high biodegradability. More research on biodegradability is still needed but on the basis of current results the environmental properties of DESs appear promising.

3.3 Aqueous choline chloride:urea

CC:U or reline is one of the most commonly used DESs (Longo & Craveiro 2018) and it can be used for example to non-hydrolyzing cellulose treatment. (Sirviö et al. 2015, Tenhunen et al. 2018) Its structure is presented in Figure 2.

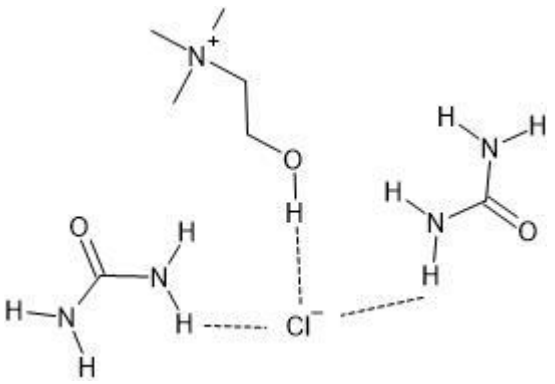

Figure 2. Structure of CC:U DES.

CC:U is a hygroscopic mixture which absorbs water from air. Meng et al. (2016) showed that in 48 hours CC:U can absorb 5.5 wt.% water from atmosphere. Hammond et al. (2017) investigated changes in CC:U DES nanostructure with different water proportions by neutron total scattering and empirical potential structure refinement. As DESs consist of coordinating, hydrogen-bonding ions and molecules they are remarkably hygroscopic and soluble to water.

Hammond et al. (2017) identified the points of hydration which change the DES-water system structure. When the water proportion increases, the DES interactions weaken

continuously but not linearly. The first discontinuity point in intermolecular coordination was observed with water content of 6.5 wt.% (Hammond et al. 2017). After this point, the best electrochemical properties of CC:U start to disappear (Du et al. 2016). Half of the pure DES structure is preserved with 41.5 wt.% water so that DES resist hydration up to this limit and water acts as a part of slightly ordered hydrogen-bonding network, mainly interacting with choline-cations. DES-water interactions increase corresponding to increasing hydration except that choline-water correlation which increases super stoichiometrically. Water engaging into hydrogen bond networks explains the buffer property towards hydration. (Hammond et al. 2017)

Second transition point is around 51 wt.% when choline-choline interactions increase and number of water molecules solvating choline decreases. With larger water proportions the DES-DES interactions fade, and water-DES interactions intensify. (Hammond et al. 2017) Diffusion coefficient of DES changes only after water wt.% exceeds 50% which supports theory that water molecules are incorporated between CC:U network (Zhekenov et al. 2017) At this point the water-water interactions are at same level than in pure water which means that the system is no longer DES, but an aqueous solution of individual DES components. (Hammond et al. 2017, Shah & Mjalli 2014, Zhekenov et al. 2017). Hammond et al. suggest that the mechanism for transition of hydrated DES to aqueous solution of DES is formation of solvent-separated ionic cluster regime between 5.5 wt.% and 51 wt.% water, which allows DES to resist solving to water until overcrowding limit is reached.

With water contents < 1 mol fraction, there is a slight increase in strength of choline-urea hydrogen-bonds (Hammond et al. 2017, Meng et al. 2016) even though all other DES interactions are weakened (Meng et al. 2016). Hammond et al. suggest that this strengthening intermolecular bond is the reason why DES systems with one molar equivalent of water do not show reduction in viscosity. Most of the nanostructure remain unchanged with one molar equivalent of water yet water contributes the nanostructure causing alteration in physico-chemical properties like viscosity and melting point (Meng et al. 2016). (Hammond et al. 2017)

3.4 DES polarity

The intermolecular solute-solvent interactions and solvent polarity are important factors when trying to understand the solvent effects on different reactions and processes. The problem of determining these parameters lies in the variety of possible interactions. Polarizability, dipole moment, charge, HBA and HBD abilities and hydrophobic forces, for example, can be responsible for interactions in the system. This leads to difficulties in describing the solvents effects with macroscopical physical parameters. (Reichardt 2005). The term polarity is slightly problematic and even in IUPACs glossary the solvent polarity is considered as a rather limited term describing the solvents overall solvation capability including all specific and non-specific interactions. (Muller 1994) Multiparameter models have been then developed to describe the overall polarity through several parameters describing the different elements of the overall polarity. (Reichardt 2005)

3.4.1 Solvatochromic method

Hydrogen bond strengths between free and bonded hydrogens of solvents can be determined with solvatochromic method proposed by Kamlet & Taft (1976a, 1976b, 1977). Interactions between solute and solvent cause observable shifts in chemical equilibria which makes it possible to examine solvent polarity with UV-Vis spectroscopy (Kamlet et al. 1976a). By using different solvatochromic probes, the assessment of different parameters for the same solvent is possible. Using these parameters in a three-parameter linear solvation energy relationship (LSER) presented in Equation 1 (Kamlet & Taft 1976a) it is possible to describe the solvents physicochemical properties, reactivity etc.:

$$XYZ = XYZ_0 + s\pi^* + a\alpha + b\beta \quad (1)$$

XYZ presents a solute property: reaction rate or equilibrium constant, or intensity or position of spectral absorption. (Kamlet et al. 1977) XYZ_0 is a respective standard reference value of XYZ. (Kamlet et al. 1981) The π* parameter is used to describe the polarizability or dipolarity of the solvent, measuring its ability to stabilize a charge or a dipole with its dielectric effect. (Kamlet et al. 1977) The α parameter describes solvents ability to donate a proton in a solvent-to-solute hydrogen bond and β describes the solvents ability to accept a proton in a solute-to-solvent hydrogen bond. (Kamlet & Taft, 1976a, 1976b) Parameters π*, α and β are normalized so that they have values between

roughly 0 and 1. Terms s, a and b are coefficients which indicate the relative sensitivity of XYZ to the solvent effects. (Kamlet et al. 1983) These parameters can be determined with UV-visible spectral data by solvatochromic comparison method as the frequency of the longest wavelength electronic absorption transition is dependent on the solvent. (Reichardt & Welton 2010)

Considering the cellulose treatment, the β parameter has been observed to correlate with cellulose swelling but also β-α value has an effect. Addition of water is noted to affect β remarkably more than other parameters. (Hauru et al. 2012) Brandt et al. (2013) reported that for ionic liquids with β value under 0.8 did not dissolve cellulose. However, it should be noted that it is possible that in high polarity solvents the solvatochromic indicators are insensitive to changes in composition as the solvent-solvent interactions dominate over solvent-solute interactions (Abbott et al. 2010).

π*-parameter

The π* scale describes the nonspecific interactions, that is other than hydrogen bonding interactions. (Laurence et al. 1994). The π* parameter can be determined by measuring the chemical shift of *N,N*-diethyl-4-nitroaniline (DENA) (Dwamena & Raynie 2020, Laurence et al. 1994, Teles et al. 2017) which is the most used indicator even though the molecule has significant vibrational structure leading to a solvent-dependent shape of the absorption band. (Laurence et al. 1994) The spectrum of DENA is bathochromically shifted with increasing solvent dipolarity (Kamlet et al. 1983). By measuring the maximum wavelength of the probe in the desired solvent and normalizing the parameter with two reference solvents, π* can be calculated with Equation 2. (Teles et al. 2017) The reference solvents are cyclohexane and diethyl sulfoxide (DMSO), for which π* gets values of 0 and 1, respectively. (Kamlet et al. 1977)

$$\pi^* = \frac{\nu_{N,N(DES)} - \nu_{N,N(cyclohexane)}}{\nu_{N,N(DMSO)} - \nu_{N,N(cyclohexane)}} \quad (2)$$

where $\nu_{N,N(DES)}$ refers to the wavenumber of DENA in DES and $\nu_{N,N(cyclohexane)}$ and $\nu_{N,N(DMSO)}$ are the corresponding wavenumbers of the probe in cyclohexane and DMSO.

β-parameter

The β-parameter can be determined by comparing the absorption peak shifts of DENA and 4-nitroaniline (4NA), of which both can act as HBA in HBD solvents but only 4NA can act as HBD in HBA solvents. (Kamlet & Taft 1975) When the absorption spectra of the probe is measured with both dyes, the only difference between the datasets should be caused by hydrogen bond acceptance of the solvent. The most used pairs, DENA/4NA and 4-nitrophenol/4-nitroaniline give remarkably differing values for same solvents. Rani et al. suggest that DENA/4NA pair could be preferable as it seems to give better internal consistency for the parameters. (Rani et al. 2011) When π* is determined, β can be calculated using Equation 3 (Teles et al. 2017):

$$\beta = \frac{(\Delta v_{(DES)} - \Delta v_{(cyclohexane)}) * 0.76}{\Delta v_{(DMSO)} - \Delta v_{(cyclohexane)}} \quad (3)$$

$$\Delta v = \Delta v_{N,N} - \Delta v_{4NA}$$

$$\mathrm{v} = \frac{1}{\lambda_{max}} * 10^{-4}$$

where v represents the experimental wavenumber, λ_{max} is the maximum wavelength of the probe, $v_{\mathrm{N,N}}$ and v_{4NA} are the wavenumbers of DENA and 4NA in a solvent referred in the subscript and Δv is the chemical shift between these two in a same solvent.

α-parameter

Rani et al. (2011) pointed out that α is the most controversial parameter of the Kamlet-Taft parameters which is probably caused by lack of structurally similar probe pairs to determine it. Instead, α is often derived from Reichardt's E_{30}^{T} scale which is problematic due to polarizability/polarity effects included in E_{30}^{T}. These effects are removed from α by utilizing π*, thus making the α value dependant on π* values and errors. (Rani et al. 2011)

Instead of deriving α from E_{30}^{T} it can be calculated with solvatochromic comparison method of two probes with different abilities for hydrogen bonding, for example. p-nitrophenol and Reichardt's dye. The absorption spectra of these probes is measured in non-HBD solvents. When the absorption peaks of two probes in reference solvent are plotted against each other a reference line is formed. Deviation from reference line is

calculated with Equation 4 for solvents of interest and α is normalized to methanol. (Eyckens et al. 2016).

$$\alpha = \frac{v_{RD}+bv_{NP}-k}{\sqrt{b^2+a^2}} \quad (4)$$

Where v_{RD} and v_{NP} represent the maximum wavenumbers of Reichard's dye and p-nitrophenol in kiloKaisers and a, b and c are constants of the reference line ay = bx+k.

Reichardt's dye is often used to determine the α-parameter, but it is suggested that Nile red (9-(diethylamino)-5*H*-benzo[*a*]phenoxazin-5-one) would be a better alternative (Dwamena & Raynie 2020, Xia et al. 2017). Commonly used Reichardt's dye is strongly dependent on the hydrogen bond donor ability (Reichardt 1965) but also on other properties of the solvent, such as dipolarity and polarizability, hydrogen bond accepting ability (Marcus 1991, Rani et al. 2011) and solute-solvent electrostatic interactions (Znamenskiy & Kobrak 2004) and it is also poorly soluble to many solvents (Madeira et al. 2017). Some solvents can even cause complete bleaching of the probe due to protonation of the dye molecule (Dwamena & Raynie 2020). Because the best comparable results are obtained by using the same dye for all solvents it would be preferable to use a probe which is suitable for all kinds of solvents (Rani et al. 2011, Xia et al. 2018).

Ready-normalized equations

Alternatively, ready-normalized equations can be used to determine Kamlet-Taft parameters as Xia et al. (2018) did in their DES experiments. Used probes are same than with solvent-normalized method but Reichardt's dye is replaced with Nile red. In this case, π*, α and β can be determined by inserting the experimental wavelengths straight into Equations 5, 6 and 7:

$$\pi^* = 0.314 * (27.52 - v_{DENA}) \quad (5)$$

$$\beta = 11.134 - \frac{3580}{\lambda(4NA)_{max}} - 1.125\pi^* \quad (6)$$

$$\alpha = \frac{19.9657-1.0241\pi^*-v_{NR}}{1.6078} \quad (7)$$

where v is $1/(\lambda_{max} * 10^{-4})$ and λ_{max} is the wavelength of maximum absorption and the subscripts refer to a probe involved.

3.4.2 Solvatomagnetic method

Recently, solvatomagnetic method has been proposed by Laurence et al. (2014) to determine the Kamlet-Taft parameters. Since the solvatochromic method gives divergent hydrogen bond acceptance results for certain important solvents, such as water, solvatomagnetic comparison method was proposed to offer more reliable and consistent results for determining the β-parameter. In this method the ^{19}F NMR spectra is measured to observe the chemical shifts of 4-fluorophenol and 4-fluoroanisole in the concerning solvents. As the chemical shift of 4-fluorophenol is highly sensitive to hydrogen bonding of OH-group in ^{19}F NMR and 4-fluoroanisole is a non-hydrogen bonding compound, it is possible to remove non-hydrogen bonding effects from overall shift. (Laurence et al. 2014 & 2021)

To calculate β, chemical shifts of probes is first measured in non-HBA reference solvents and the negative of probe shifts are plotted against each other to form a reference line. Deviation from reference line of solvents of interest represents the contribution of the hydrogen bond to the chemical shift of 4-fluorophenol. With reference values measured by Laurence et al. (2021) β can be calculated with Equation 8:

$$\beta = \frac{[-\delta(^{19}F)_{OH}]-\{1.009-[-\delta(^{19}F)_{OMe}]\}-1.257}{3.041} \quad (8)$$

where $\delta(^{19}F)_{OH}$ is fluorine chemical shift of 4-fluorophenol and $\delta(^{19}F)_{OMe}$ is fluorine chemical shift of 4-fluoroanisole.

Especially the α-parameter has given conflicting values with solvatochromic method (Rani et al. 2011) but the HBD ability could be determined more precisely with solvatomagnetic method. (Madeira et al. 2017) Schneider et al. (1992) proposed using pyridine-N-oxide (PyO) as a probe and measuring the chemical shift δ of C2 and C4 by ^{13}C NMR. The shift could be measured with UV-Vis spectroscopy too, but the PyO absorption peak often overlaps with absorption region of many solvents (Madeira et al. 2017). The shift of PyO is not dependent of other properties than hydrogen bond donating ability (Marcus 1991). After determining the carbon peak shifts, the α can be calculated by Equation 9 (Teles et al. 2017, Schneider et al. 1992):

$$\alpha = -0.15 * d_{24} + 2.32 \quad (9)$$

where d_{24} is δ_4- δ_2.

3.5 DES and cellulose

Energy consumption in CNF production is very high when only mechanical treatments such as high-pressure homogenizers are used. Non-treated cellulose also easily clogs the homogenizers. To overcome this problem, different pretreatment methods have been developed including chemical, physical, and enzymatic methods. (Klemm et al. 2011) Combination of chemical and mechanical treatment is preferrable in disintegrating cellulose fibers as in addition to decreased energy consumption it allows formation of microfibrils with smaller widths. (Saito et al. 2006)

Many chemical modifications use halogenated chemicals and cause heavy damage on cellulose fibers by reducing DP and causing yield losses. With milder, non-modifying methods with DES solvents these problems can potentially be avoided. (Sirviö et al. 2020) It has been shown that CC:U DES does not alter the cellulose I crystalline structure or DP. (Sirviö et al. 2015, Tenhunen et al. 2018) Instead, the solvent reduces strong intra- and intermolecular hydrogen bonds of the cellulose (Wang et al. 2015) presented in Figure 3 which results in "loosening" of the hydrogen bond network (Sirviö et al. 2015). However, Tenhunen et al. (2018) noted that changes in nitrogen content of cellulose were observed after DES treatment which was suggested to originate from choline groups attached on the anionic surfaces of the cellulose with electrostatic forces. In addition to CC:U, other DESs can be used to swell cellulose fibers, for example choline chloride:imidazole (Sirviö et al. 2020) and ammonium thiocyanate:urea (Li et al. 2017).

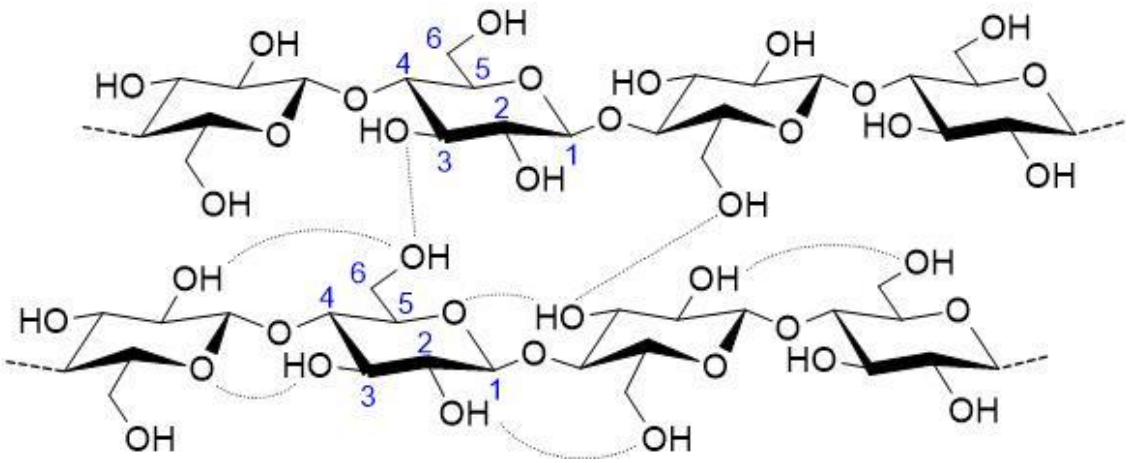

Figure 3. Inter- and intramolecular hydrogen bonds of cellulose.

CC:U based DESs has been applied on pretreatment of cellulose for nanofibrillation (Sirviö et al. 2015 & 2020, Yu et al. 2020). Sirviö et al. (2015) combined choline chloride and urea in molar ratio of 1:2 and heated the mixture in oil-bath at 100 °C for 15 minutes obtaining a clear, colorless liquid. Dried and ripped cellulose was added to solution, mixed for 2 hours, and finally washed with de-ionized water. Pretreated pulp was diluted and passed through microfluidizer. The disintegration time of pulp into DES was suggested to depend on mixing speed and the size of the cellulose pieces. When water was added to DES-cellulose mixture it changed to gel-like and swollen material but after washing no visible differences were observed between DES treated and original pulp. The yield of the DES treatment was 90%, of which the lost 10% was suggested to be mainly hemicellulose dissolved to DES. Non-treated pulp could not be disintegrated due to clogging of the microfluidizer chambers, but the DES-treated pulp flowed through without problems. Produced material was homogenous, turbid and gel-like. (Sirviö et al. 2015)

TEM pictures showed that nanofibrillated cellulose formed a web-like structure which consisted of 2-5 nm wide individual nanofibers and nanofiber aggregates, of which most were 15-30 nm wide, relatively small bundles which consist of a few individual nanofibers. Larger bundles of 50-200 nm were observed only with the mildest mechanical treatment. Considering the mechanism of nanofibrillation it was observed that many individual nanofibers had started to peel off the bundle, but they did not detach completely in milder treatments. Sirviö et al. (2015) concluded that that nanofibrillation occurs through individual nanofibers peeling off from bundle surfaces of larger particles breaking down. Transmittance of nanofiber suspension was observed to decrease with longer treatment. CC:U treatment did not alter the DP of the cellulose which allows the process to be called non-hydrolytic. A weak additional band was observed in DES-pulp in DRIFT -spectra which might be caused by urea and cellulose forming a carbamate bond in elevated temperatures. (Sirviö et al. 2015)

4 EXPERIMENTAL

Due to hygroscopic character of CC:U DES the water uptake is inevitable (Du et al. 2016). Drying processes of solvent would also increase the energy consumption and therefore it would be more practical to use aqueous CC:U especially in industrial applications. In this work, properties and treatment efficiency of CC:U was studied with different molar ratios and water contents. The water contents were related to CC so that for each set of samples with same CC:U molar ratio (1:2, 1:1, 2:1) the tested water contents were 2, 4, 6, 8 and 10%, related to CC so that the name of the samples are in a form CC:urea:water. Analysis of samples 1:1:0, 2:1:0 and refUrea were limited as they were not liquid in room temperature. Deionized water was used unless otherwise stated.

4.1 Cellulose treatment

DESs for the experiments were prepared from water, choline chloride (98.0%) from Algry Quimica S.L. and urea (99.0-100.5%) from Sigma-Aldrich. Since both CC and urea are hygroscopic and the chemicals were not dried or stored in moisture-free conditions, even the DESs with no added water contained some water, which was confirmed later in NMR analysis. DESs were formed by combining the substances in to a 250 ml Schott bottle according to Table 1. Reference samples were pure water, water with pH adjusted to 10, CC/water, CC/ water with pH adjusted to 10 and water/urea. Solvent pHs were adjusted with 0.1 M sodium hydroxide from FF Chemicals. Dry pulp sheets were commercial softwood kraft pulp (MetsäFibre, Finland). Moisture content of the pulp was measured with Ohaus MB23 moisture analyzer to correct the weighted pulp amount to dry mass. Solvents were mixed with magnetic stirrer in 100 °C oil-bath until a clear liquid was obtained. Samples with CC:U molar ratio 1:0.5 were not completely clear even in 100 °C, especially sample 1:0.5:0 which was hardly a liquid but rather a turbid sludge. This was expected as the melting points for 1:2:0, 1:1:0 and 2:1:0 CC:U DESs are 12.2, 55.7 and 142.5 °C, respectively (Morais et al. 2018).

Table 1. DES recipes for cellulose treatment.

Sample name	Water mol-%/wt.%	Choline chloride (g)	Urea (g)	Water (g)	Pulp (g)
1:2:0	0/0	26.88	23.12	0	1.0852
1:2:2	0.40 / 0.12	23.61	20.31	6.09	1.0858
1:2:4	0.57 / 0.22	21.04	18.10	10.85	1.0822
1:2:2	0.67 / 0.29	18.98	16.33	14.68	1.0822
1:2:8	0.73 / 0.36	17.29	14.88	17.83	1.0850
1:2:10	0.77 / 0.41	15.88	13.66	20.47	1.0822
1:1:0	0 / 0	34.96	15.04	0	1.0812
1:1:2	0.50 / 0.15	29.62	12.74	7.64	1.0825
1:1:4	0.67 / 0.26	25.70	11.05	13.25	1.0824
1:1:6	0.75 / 0.35	22.69	9.76	17.55	1.0826
1:1:8	0.80 / 0.42	20.31	8.74	20.95	1.0830
1:1:10	0.83 / 0.47	19.39	7.91	23.70	1.0839
1:0.5:0	0 / 0	41.15	8.85	0	1.0834
1:0.5:2	0.57 / 0.18	33.95	7.30	8.75	1.0832
1:0.5:4	0.73 / 0.30	28.89	6.21	14.90	1.0830
1:0.5:6	0.8 / 0.39	25.14	5.41	19.45	1.0838
1:0.5:8	0.84 / 0.46	22.26	4.79	22.96	1.0837
1:0.5:10	0.87 / 0.51	19.97	4.29	25.74	1.0839
refCC 1:0:2	0.67 / 0.20	39.75	0	10.25	1.0823
refUrea 0:1:2	0.67 / 0.37	0	31.26	18.74	1.0842
refWater	1.00	0	0	50.00	1.0847
refWaterNaOH (pH 10)	1.00	0	0	50.00	1.0823
refCCNaOH (pH 10)	0.67 / 0.20	39.75	0	10.25	1.0832

When the DESs had cleared or no visible change was anymore observed (maximum 30 minutes), 1.00 g of dry pulp was added to the solvent. Pulp was ripped to roughly 1 cm^2 pieces and treated at 100 °C for 1 hour under mixing. For the first 5 minutes the mixing speed was 150 rpm after which it was increased to 500 rpm. For the most viscous mixture 2:1:0 the magnetic bar was not able to stir the suspensionr. After 1 hour treatment additional 20 ml water was poured into the suspension and mixed well into the DES-pulp mixture. The mixture was filtered with Buchner filtration unit using 5-13 µm filtration ␣. Pulp was washed with 1000 ml of water which was poured on pulp in three parts.

4.1.1 Cellulose treatment without mixing

Surprisingly, the best fiber swelling results were observed with tripled 1:0.5:0 experiment in which the stirrer got stuck. Magnetic stirrer could not handle larger amount of DES and got stuck after introducing the pulp. Therefore, the effect of stirring on fiber swelling was further investigated.

As it was noticed that the clumped 1:0.5:0 sample resulted in the highest degree of fiber swelling, treatments without mixing were also conducted for other samples in original batch size of 50 g. Samples without any added water (1:2:0, 1:1:0 and 1:0.5:0), samples with the highest water content (1:2:10, 1:1:10 and 1:2:08) and refWater were chosen to be tested without mixing. The treatment procedure was exactly the same than with original DES treatment samples but without mixing. The fiber properties were analyzed with Valmet FS5 and the results were compared to samples made with the mixing treatment.

4.2 Fiber analysis

4.2.1 Fiber properties

The DES treated and washed pulp was scraped to a container and moisture content of the pulp was measured with Ohaus MB23 analyzer to calculate the yield. Fiber properties of the treated samples were analyzed using FS5 image analyzer. The analysis was conducted as triplicates and the results were averaged. A reference sample analysis of non-treated pulp was prepared according to ISO5263-1:2004(E) standard.

4.2.2 Diffuse reflectance infrared Fourier transform spectroscopy

The characteristic Fourier-transform infrared spectroscopy (FTIR) absorption spectra of cellulose consist of OH stretching at 4000-2995 cm^{-1}, CH stretching at 2900 cm^{-1}, HCH and OCH in-plane bending vibrations at 1430 cm^{-1}, CH deformation vibration at 1372 cm^{-1} and COC, CCO and CCH deformation modes and stretching vibrations at 900 cm^{-1}. (Sirviö et al. 2015, Oh et al. 2005, Proniewicz et al. 2001, Schwanninger et al. 2004, Ivanova et al. 1989). The OH stretching spectra includes intramolecular hydrogen bonds O(2)H…O(6) (3455-3410 cm^{-1}) and O(3)H…O(5) (3375-3340 cm^{-1}) and one intermolecular hydrogen bond, O(6)H….O(3') (3310-3230 cm^{-1}) (Schwanninger et al. 2004). The FTIR spectra can be used to determine changes in hydrogen bonding of

cellulose hydroxyl groups by fitting peaks for these three hydrogen bond types in the OH stretching area. (Wan et al. 2015, Zhu et al. 2020). However, it should be noted that bands from other origins may also appear on this range (Schwanninger et al. 2004).

Chemical characterization for pulp samples were performed using Attenuated total reflection infrared (ATR-IR) spectroscopy. The spectra were collected with a Bruker Tensor II FT-IR spectrometer with a Hyperion 3000 FT-IR microscope. The dried pulp was pressed with a manual hydraulic jack to form a tab. The spectra were measured with 40 scans for each sampled in the 600-4000 cm^{-1} range with resolution of 2 cm^{-1}. Determination of changes in hydrogen bonding of OH-groups was made with peak fitting software Fityk. Peaks were located by setting the initial peak guess on the supposed peak rages and defining the specific peak by automatic fitting with Levenberg-Marquardt method as Gaussian curve. The bond energies (E_H) were calculated with Equation 10 and bond lengths (R) with Equation 11. (Zhu et al. 2021, Wan et al. 2015)

$$E_H = \frac{1}{\mathrm{k}}\left[\frac{v_0 - v}{v_0}\right] \tag{10}$$

where k is constant (3.82×10^3 kJ^{-1}), v_0 is the standard free hydroxyl (–OH) frequency (3650 cm^{-1}) and v is the sample hydroxyl (–OH) frequency.

$$\Delta \mathrm{v}(cm^{-1}) = 4.43 * 10^3(2.83 - R) \tag{11}$$

where $\Delta v = v_0 - v$, v_0 is stretch vibrational frequencies of hydroxyl at 3600 cm^{-1} and v is the sample hydroxyl (–OH) frequency.

4.2.3 Cellulose reactivity

Reactivity of DES treated cellulose was revealed by introducing carboxylate groups into cellulose with (2,2,6,6-tetramethyl-piperidin-1-yl)oxyl (TEMPO) oxidation and then determining the amount of acidic groups by conductometric titration. (Sirviö et al. 2014) TEMPO-oxidation reaction occurs on the surface of the fibers which introduces a negative charges but does not remarkably alter the fiber structure. (Saito & Isogai 2005) TEMPO-treatment loosens the adhesion forces, introduces electrostatic repulsions between microfibrils and increases the charge repulsion between fibrils. When non-dried cellulose is TEMPO-oxidized, it can be disintegrated into individual nanofibrils unlike

with dried cellulose because drying causes irreversible changes to the cellulose structure. (Saito et al. 2006)

Three different pulps were chosen for this experiment: 1:0.5:0 as it gave the best fiber swelling results, 1:0.5:10 to observe effect of water in DES and pure water was chosen as a reference. The samples were prepared according to Table 3 but in three times bigger batches. Sample 1:0.5:0 did not success in tripled batch as the magnetic stirrer could not handle increased mass and after 10 minutes of treatment the solution clumped, and the stirrer got stuck. DES treatment with 1:0.5:0 was re-made in a 600 ml decanter with standing propeller mixer and a non-airtight lid. Amount of rinsing water was also tripled. Otherwise, the procedure was similar than with other treatments. Chemicals used were 0.05 M phosphate buffer with pH 7.00 (FF-Chemicals), technical grade NaClO (VWR), (2,2,6,6-tetramethyl-piperidin-1-yl)oxyl (>98.0%, GC Chemicals) and $NaClO_2$ (80%, Sigma-Aldrich).

DES -treated samples were kept in closed containers at 4 °C for 3 days. After that, dry matter contents of the pulps were measured (20.0% for refWater, 30.08% for 1:0.5:10 and 17.5% for 1:0.5:0) and 2.00 g of pulp as dry mass (10.00 g refWater, 6.49 g 1:0.5:10, 11.43 1:0.5:0) was weighed to a measuring glass which was then filled to 180 ml with 0.5 M phosphate buffer (pH 7). The mixture was poured in a round-bottom flask equipped with magnetic stirrer and placed in 60 °C oil bath. A reflux condenser was placed on the flask. Next, 0.032 g of TEMPO reagent was added to flask. NaClO buffer solution was prepared by adding 1.5 ml 1.34 M NaClO to 1.63 ml phosphate buffer. Mixture of 3.13 ml of NaClO solution and 2.26 g $NaClO_2$ (dissolved into 10 ml phosphate buffer) were pipetted to flask one drop at time. Mixture of 3.13 ml of NaClO solution and 2.26 g $NaClO_2$ (dissolved into 10 ml phosphate buffer) were pipetted to flask one drop attime. After 24 hours reaction, 1 ml of ethanol was added to stop the reaction. Treated pulp was washed with water until the conductivity was under 10 µS/cm. Pulp treated with 1:0.5:0 was very fast to be filtered, but it needed one extra washing before reaching the required conductivity. Pulp treated with 1:0.5:10 was only a bit slower than 1:0.5:0. Instead, refWater was very slow to filter but it required only three washes. After washing pulps were sealed in containers and stored in 4 °C overnight.

A conductometric titration was made as duplicates.as duplicates. Dry matter content of the washed pulp was measured (12.5% refWater, 10.3% 1:0.5:10, 13.2% 1:0.5:0) and 0.5

of absolute pulp was weighed to a titration cup. Next, 10.00 ml of 0.01 M NaCl solution was added to acupa beaker which was filled to 70 g with water and pH of the mixture was adjusted to 3 with 0.1 M HCl. The titrant was 0.05 M NaOH solution and automatic . Automatic titrator Mettler Toledo M437 was used.

Obtained titration curves were divided to three parts according to Figure 3. Microsoft Excel was used to determine trendline functions of the first and last part to obtain curve slopes and constants and the average of horizontal data points were calculated. The amount of acidic groups was then determined according to Equations 12, 13 and 14:

$$N = \frac{V_1 - V_0}{m} \cdot c_{NaOH} \tag{12}$$

$$V_0 = \frac{b - average\ of\ the\ middle\ part}{k} \tag{13}$$

$$V_1 = \frac{(average\ of\ the\ middle\ part) - b}{k} \tag{14}$$

in which N is the amount of acidic groups (mmol/g), V_0 and V_1 are the volumes of added NaOH before the first and after the second crosspoint, b is the constant of trendline, k is slope of the trendline, c_{NaOH} is the concentration of NaOH titrant (mol/l) and m is the absolute mass of the pulp (g).

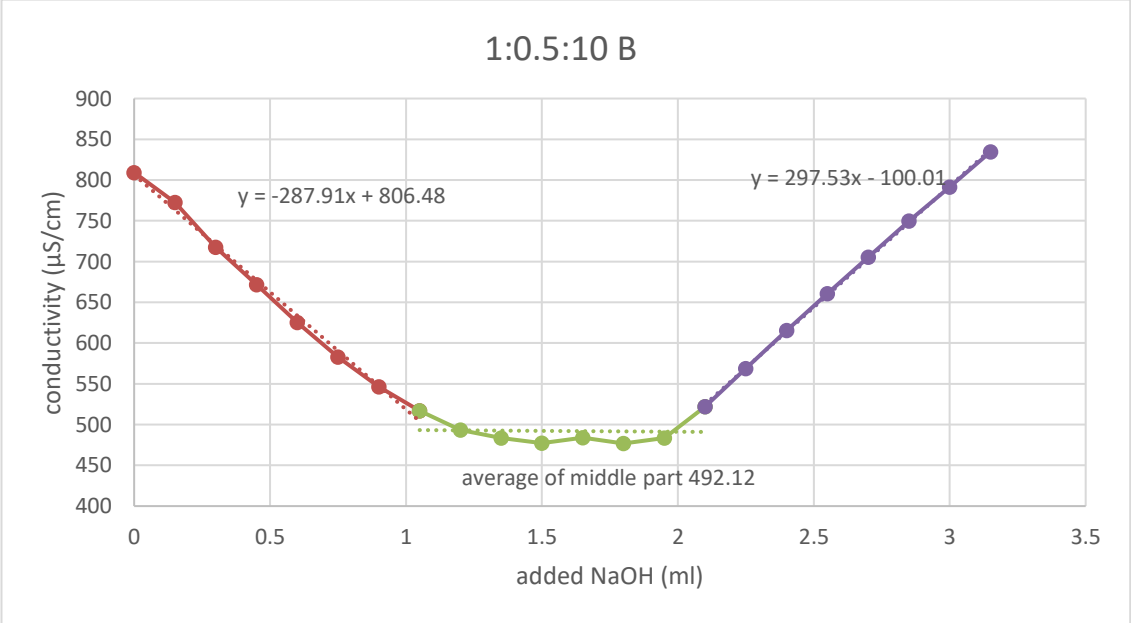

Figure 4. Conductometric titration curve of 1:0.5:10 B with trendlines.

4.2.4 Nanofibrillation

Nanofibrillation of DES treated pulps was performed with a two-chamber microfluidizer Microfluidics M-110EH-30. Pulp from DES treatments were dried in 105 °C oven overnight and weighed. Dry weight of 1:2:0 cellulose was 0.47 grams, and it was mixed into 500 ml of water (0.094%) and homogenized with Ultra-Turrax mixer for 5 minutes. The homogenized solution was driven through a microfluidizer, three times with 1200 bar with 400 and 200 chambers and 2 times with 1500 bar through 400 and 100 chambers. The resulting mixture was grainy and did not seem properly dispersed. Similar nanofibrillation was made with 0.59 g of 1:2:10 in 600 ml of water (0.098%). The nanofibrillated solution was centrifuged to find out the degree of nanofibrillation. In the analysis, the nanofibrillated cellulose stays in the liquid layer and non-fibrillated fibers sink to the bottom. The dry matter content (DMC) after nanofibrillation was 0.0778% for 1:2:0 and 0.087% for 1:2:10. After centrifugation the DMC on the upper liquid layer was 0.0283% for 1:2:0 and 0.0286% for 1:2:10.

4.3 DES properties

New batches of DESs were prepared using a half the quantity mentioned in the Table 1 for determination of DES properties. All samples were weighed into 100 ml Schott bottles and put to oven at 100 °C for 20 hours. After 20 hours all samples except 1:0.5:0 had melted and formed a clear liquid. Sample 1:0.5:0 was liquid from the bottom but solid on the top layer. Pictures of the samples are presented in Figure4. Sample 1:1:0 started to solidify rapidly when the taken to room temperature.

Figure 5. Pictures in rows 1-3 are taken after 5 minutes from taking samples from 100 °C oven to room temperature. Row 1: CC:U samples with molar ratio 1:2:X with increasing water content from left to right. Row 2: CC:U samples with molar ratio 1:1:X with increasing water content from left to right. Row 3: CC:U samples with molar ratio 1:0.5 with increasing water content from left to right.

4.3.1 Viscosity, pH and conductivity

Viscosities of the solutions were measured with TA Instruments Discovery HR-1 hybrid rheometer using flow sweep procedure with cone diameter of 40 mm and cone–plate angle of 1.999° and step time of 35 s. Viscosities were measured at 20 °C for all samples which were liquid in room temperature (all except 1:1:0, 1:0.5:0 and refUrea) and for all samples at 100 °C. Even though 1:2:0 was liquid at room temperature it was too viscous for the rheometer to be measured. DES 1:0.5:0 was too viscous to measure even at 100 °C.

Conductivity and pH were measured at 23 °C from all samples which were in the liquid form (~23 °C). RefUrea was a supercooled liquid and solidified, if the bottle was shaken

at room temperature, which caused some challenges for measurements which required stirring. RefUrea sample was heated to 50 °C to avoid crystallizing during the measurements of pH and conductivity and its viscosity was only measured at 100 °C.

4.3.2 Solvatochromic method

UV-Vis spectra was measured for all samples which were liquid in room temperature with VWR UV-6300PC Double Beam Spectrophotometer. Used dyes were 4-nitroaniline (≥99%) from Sigma-Aldrich, N,N-diethyl-4-nitroaniline (98%) from Apollo Scientific Ltd. and Nile Red from Tokio Chemical Industry Co. Structures for solvatochromic and solvatomagnetic probes are presented in Figure 5. Reference solvents were dimethylsulfoxide (>99.0%) from GC Chemicals and cyclohexane (99%) from RCI Labscan. Measurements were made with quartz cuvettes for Nile red and DENA and water was used for background subtraction. Spectra for 4NA were measured without reference sample. Baseline correction for all samples was made with 1:2:2.

DENA and 4FA spectrums were measured first with 2 mg/4 ml concentration as in Teles et al. (2017) experiment. The concentration was found to be too high for both dyes, but 0.10 mg/4 ml gave clean spectrum peaks. The spectra were measured in 300-700 nm range. The preparation of samples was made by weighting dyes into a glass bottles and the solvents were poured on dye crystals. The mixtures were let to solve at 80 °C oven for 3 hours, except cyclohexane which was at 60 °C oven due to its lower boiling point.

Measurement of Nile red spectra turned out to be challenging as even 0.1 mg/ 4ml did not dissolve to DESs even with heating and stirring. Spectra were measured with 0.01 mg/ 4 ml concentration. Sample were prepared by letting Nile red to dissolve for 2 hours at 90 °C with vigorous mixing, which led to visible particles disappear and the solution turned light violet. The spectra gave a sufficient spectrum peak for all samples except for refWater whose spectrum was so weak that the finding the maximum absorbance value became uncertain.

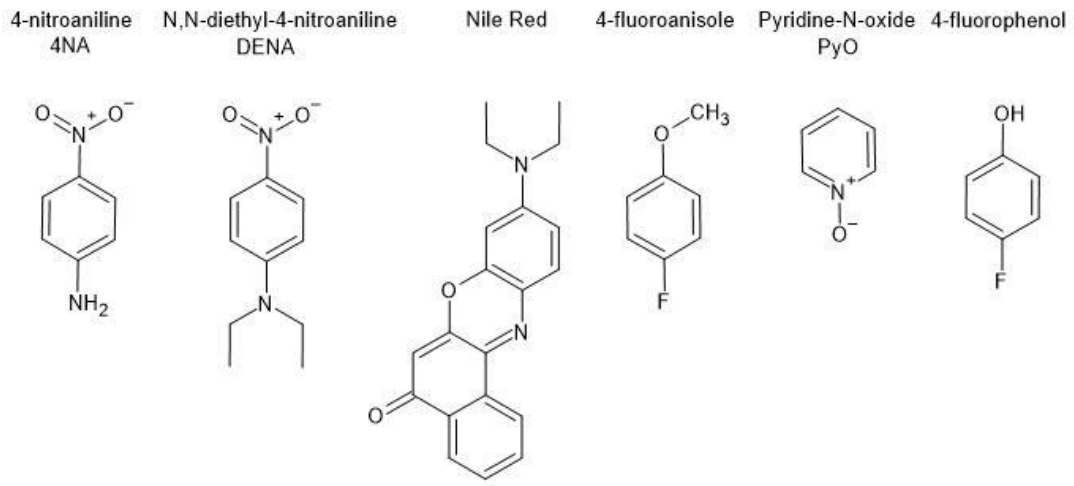

Figure 6. Chemical structures of solvatochromic and solvatomagnetic probes used in this work.

References for the calculations were made by measuring the UV-spectra of DENA, 4NA and Nile red, in DMSO and cyclohexane. DMSO dissolved all dyes rapidly unlike cyclohexane. Cyclohexane samples were put into 65 °C oven for 2 hours. Nile red containing sample turned goldish, and DENA dissolved but 4NA particles had stayed on the bottom of the sample container. 4NA sample was heated to 60 °C on hot plate and magnetic stirrer was added. After 1 hour of mixing the 4NA crystals had dissolved but the solution was still clear of color. The sample was heated and mixed again and immediately analyzed with UV-spectrometer because, when the sample cooled, furry/fiber-like bright yellow particles started to precipitate in the solution with 0.1mg/4ml concentration tested. However, this behavior was not observed with 4NA concentration of 0.01 mg/ 4ml.

4.3.3 Solvatomagnetic method

Used probes were 4-fluoroanisole (≥97.0%, GC Chemicals), 4-fluorophenol (> 99.0%, Tokyo Chemical Industry Co.) and pyridine-N-oxide (95%, Sigma-Aldrich). Nuclear magnetic resonance (NMR) measurements were carried out on a Bruker Avance III 600 spectrometer by pulse sequence method. Spectrums were recorded with Waltz proton decoupling. Deuterated chloroform with 0.03% tetramethylsilane (99.80% D, Eurisotop) and trifluoroacetic acid (>99.0%, Tokyo Chemical Industry Co.) were used as internal standards. Reference measurements were performed at 25 °C.

For determining the β-parameter, 2 mg of 4-fluoroanisole was dissolved to 2 ml of DES. The 4-fluorophenol crystals did not dissolve well but after 12 hours in 80 °C oven visible particles had dissolved. Chemical shift of 4-fluoroanisole was measured with concentration of 10 µl/ 2 ml DES but 2 hours heating 80 °C oven was needed to dissolve the floating droplets into DESs with larger water content. Reference solvent values from Laurence et al. (2021) study were used in this work. In ^{19}F measurements used frequency was 564.7 MHz, spectral width was 29.9175 ppm, relaxation delay 10 s and number of scans 64.

For determination of α, 47.55 mg of PyO was dissolved into 2 ml of DES. Mixtures were kept in 40 °C oven for 12 hours to dissolve PyO. DES 1:2:0 needed additional 2 hours in 80 °C to dissolve all PyO particles. For ^{13}C measurements used frequency was frequency 150.9 MHz, spectral width was 240.0744 ppm, relaxation delay 2 s and number of scans 128.

5 RESULTS AND DISCUSSION

5.1 Cellulose treatment

5.1.1 Fiber properties of DES pretreated cellulose

FS5 fiber image analysis results of width, length, curliness, kinks, kink angles and fines are presented in Table 3. The detailed results can be found in in Appendix 1. With more viscous solvents, the fibers seemed to swell more but that is probably due to solvent sticking on the pulp pieces during the treatment. The fibers treated with DES having the highest water content had a sharper and denser appearance after washing on the filter paper. However, the measured dry matter contents of samples varied from 22.4% to 40.0% which probably caused differences in the visual appearance of the samples.

Table 2. Fiber properties of DES treated pulps.

Sample name	Fiber width (µm)	Fiber lenght (mm)	Curl (%)	Kink (1/m)	Kink angle (deg)	Fines (%)
1:2:0	36.81	1.818	15.49	4060	31.09	9.77
1:2:2	37.05	1.884	15.77	4015	30.91	8.05
1:2:4	37.22	1.848	17.14	4194	32.16	8.21
1:2:6	36.62	1.831	16.05	4086	31.31	8.17
1:2:8	36.77	1.832	16.62	4116	31.64	7.34
1:2:10	36.99	1.865	16.26	3999	31.39	7.87
1:1:0	37.2	1.846	16.33	4193	31.63	9.49
1:1:2	37.1	1.870	16.36	4082	31.96	7.21
1:1:4	36.94	1.856	16.16	4115	31.84	7.88
1:1:6	36.85	1.870	16.93	4277	32.49	7.04
1:1:8	37.09	1.826	17.38	4271	33.34	8.62
1:1:10	36.88	1.865	16.32	4115	31.74	7.36
1:0.5:0	37.56	1.858	16.39	3916	32.55	7.48
1:0.5:2	37.12	1.877	15.85	4053	31.53	7.65
1:0.5:4	37.09	1.847	16.71	4100	32.77	8.37
1:0.5:6	36.71	1.843	15.79	3940	31.33	8.02
1:0.5:8	36.9	1.848	15.61	3854	31.57	8.12
1:0.5:10	37.12	1.851	17.36	4154	32.62	7.67
refCC	37.04	1.865	15.92	4043	31.62	7.09
refUrea	36.98	1.851	16.01	3884	30.61	7.84
refWater	37.00	1.795	18.34	4398	32.83	8.63
Non-treated Pulp	36.03	1.839	15.23	4065	31.43	10.44
refWater NaOH	36.70	1.766	19.02	4504	34.78	9.26
refCCNaOH	36.98	1.857	16.24	4082	31.99	7.42

The most interesting property of fibers was their width which indicated the loosening of the fiber structure and confirmed the swelling (Li et al. 2017). Treatment of fibers with all DESs increased the fiber width 0.97 µm on average compared to non-treated reference pulp which had fiber width of 36.03 µm. Water content did not seem to affect swelling remarkably as seen in Figure 6. However, a slightly decreasing trend in fiber width appears with increasing water content. Surprisingly, even boiling in pure water increased the fiber width with 0.97 µm, which is in fact more than with DES 1:2:0 (0.78%) which has been used in nanocellulose production (Sirviö et al. 2015). The best degree of swelling was achieved with DES 1:0.5:0 which increased the fiber width to 37.12 µm (4.2%).

Reference samples with pH adjusted to 10 did not perform as well as many of the DESs. The results indicate that aqueous DESs still promote the cellulose swelling.

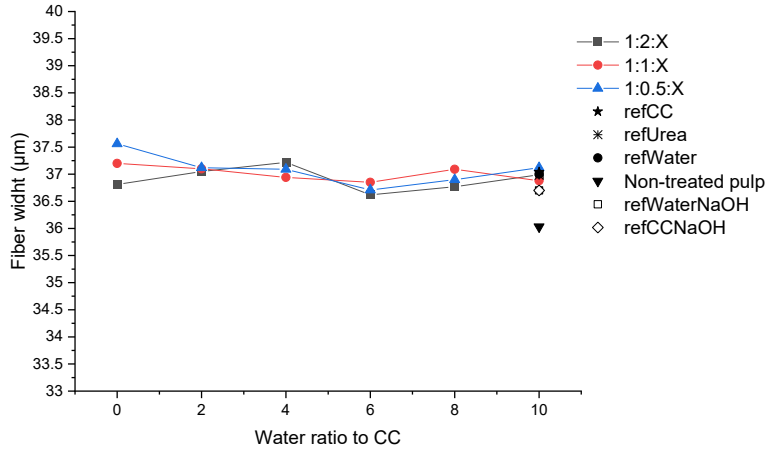

Figure 7. Effect of water content of DES on fiber width.

Other interesting property is the fiber length as the treatment of cellulose should swell the fibers but not cut or break them or reduce DP. DES treated pulps had no remarkable decrease in fiber length compared to non-treated pulp as seen in Figure 7. Reference sample refCC with NaOH had the shortest fiber length. Interestingly, pure water reference had the second shortest fiber length. Fiber length and width did not correlate which could indicate that the fiber length has naturally greater variance and effect of DES treatment on it is negligible.

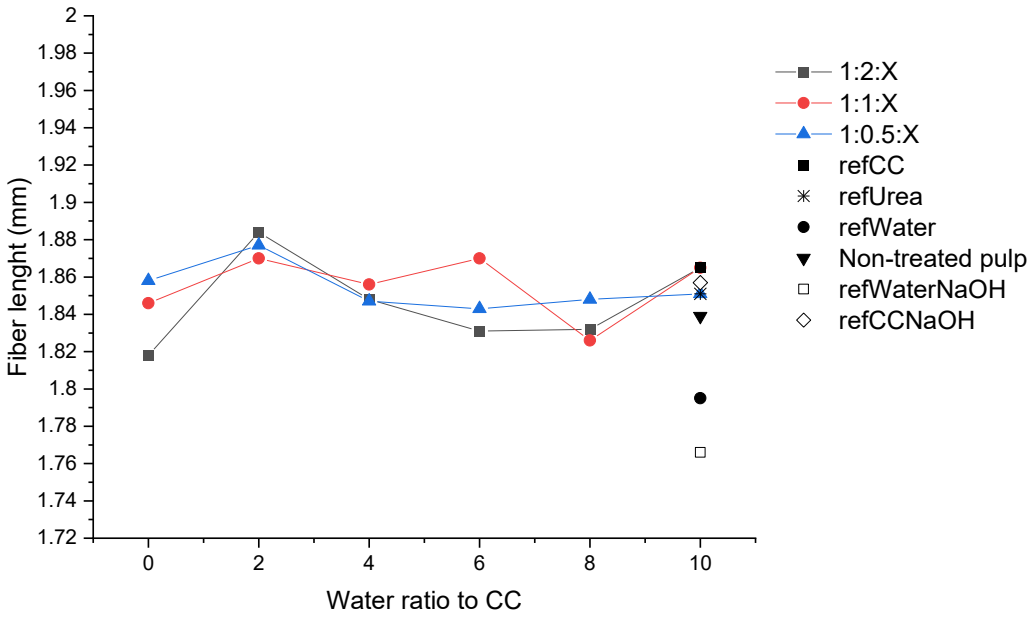

Figure 8. Effect of water content of DES on fiber length.

Harsh treatments may cause fiber deformations, such as increase in the number of kinks and curls on cellulose fibers making them susceptible to shortening (Chandra et al. 2019). Curls and kinks decrease the segment activation in fiber resulting in decreased tensile stiffness indices but in increased tear and fracture toughness indices. Even though the strength of the single fiber remains unchanged, the changed structure of the network allows stress to distribute to larger area and thus increases the fiber network strength. (Joutsimo et al. 2004)

The number of curls increased for all the treated pulps, especially for refWater and refWater with NaOH as seen in Figure 8. Water samples had also more kinks as seen in Figure 9. Other samples had kinks and kink angles close to non-treated pulp. RefWater had high kink angles as seen in Figure 10. RefWaterNaOH had again the greatest deformations. One explanation for water samples having a larger content of deformations might be related to mixing as DESs, refUrea and refCC had clearly higher viscosity. Even though the mixing speed of magnetic stirrer was same in all experiments it is possible that actual speed of the mixture was remarkably lower for viscous solvent-pulp mixtures. Therefore, standing mixer should probably be used in further experiments to rule out the influence of mixing speeds on the results.

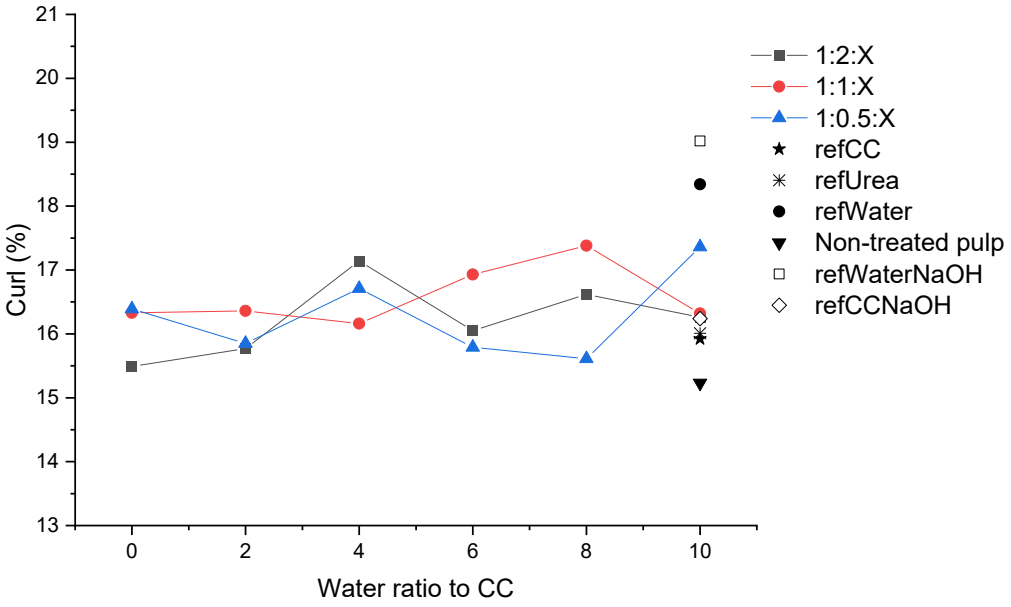

Figure 9. Effect of water content of DES on fiber curliness.

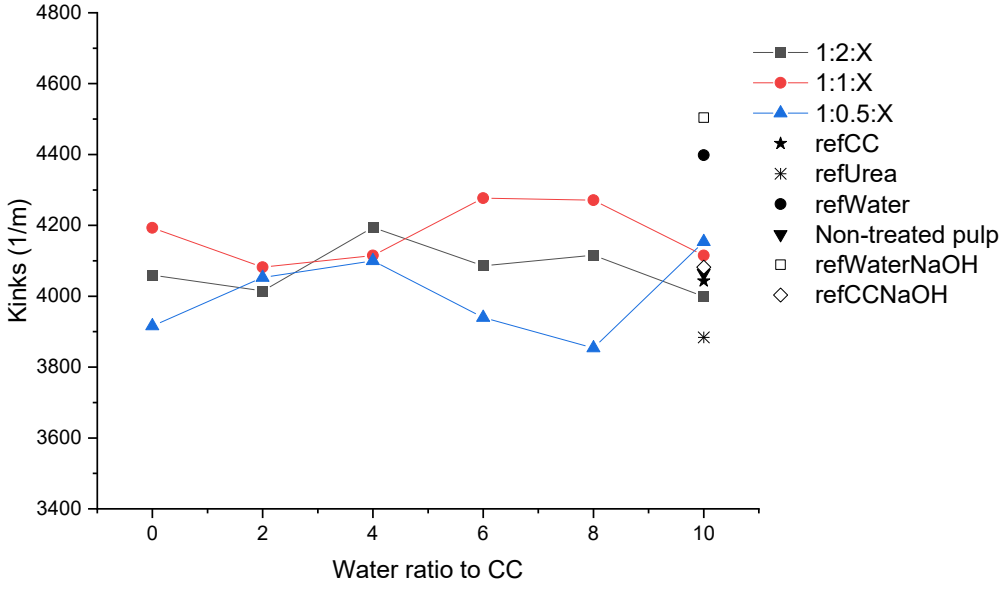

Figure 10. Effect of water content of DES on fiber kinks.

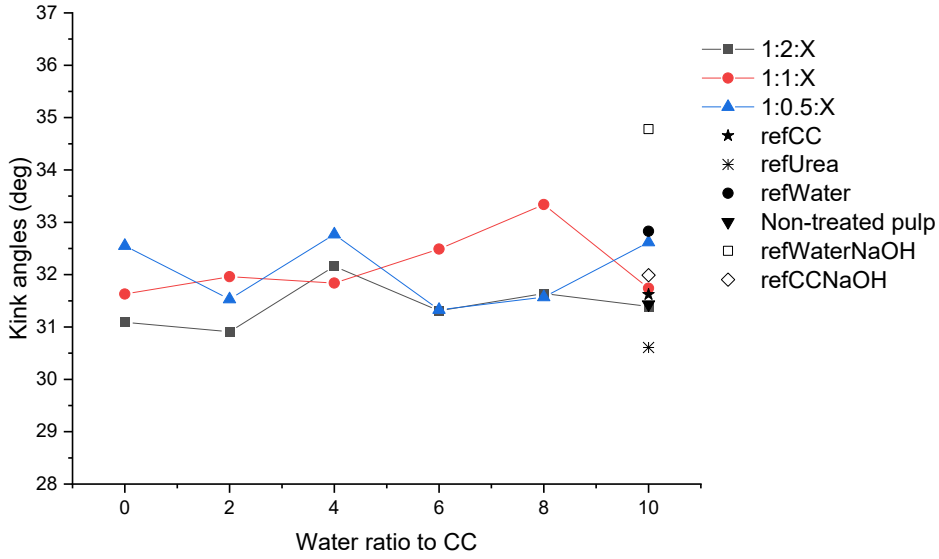

Figure 11. Effect of water content of DES on fiber kink angles.

Non-treated pulp had the largest content of fine particles (10.44%). DESs 1:2:0 and 1:1:0 had also clearly larger fine contents than other samples. The number of fines did not have a clear trend as a function of water content of DESs like other fiber parameters, Figure 11. Instead, fine contents were correlated with fiber length so that shortening of fibers increased fines content as seen in Figure 12. This was expected as the small fiber fragments are calculated as fines by FS5.

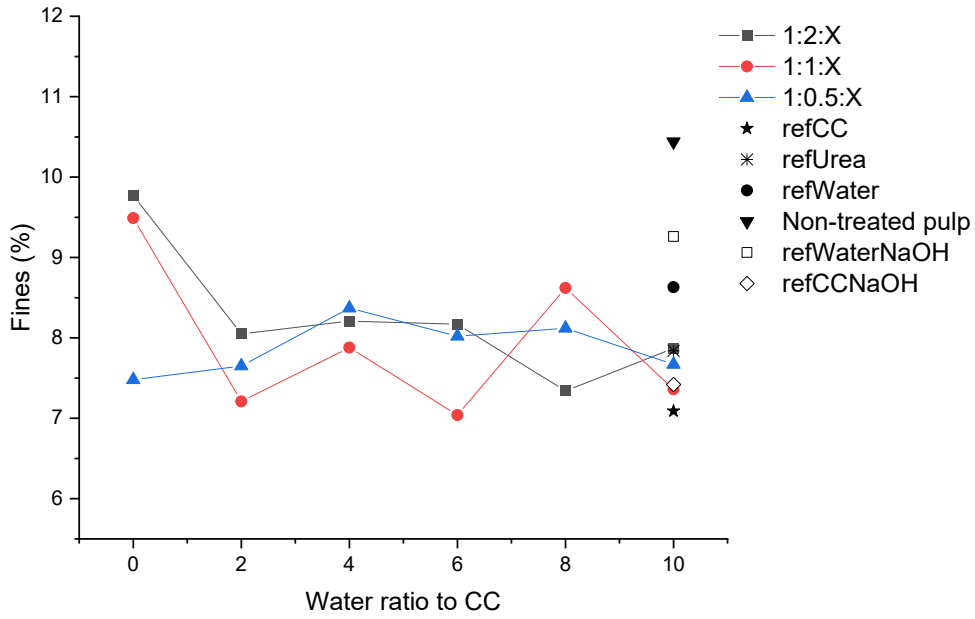

Figure 12. Effect of water content of DES on pulp fines.

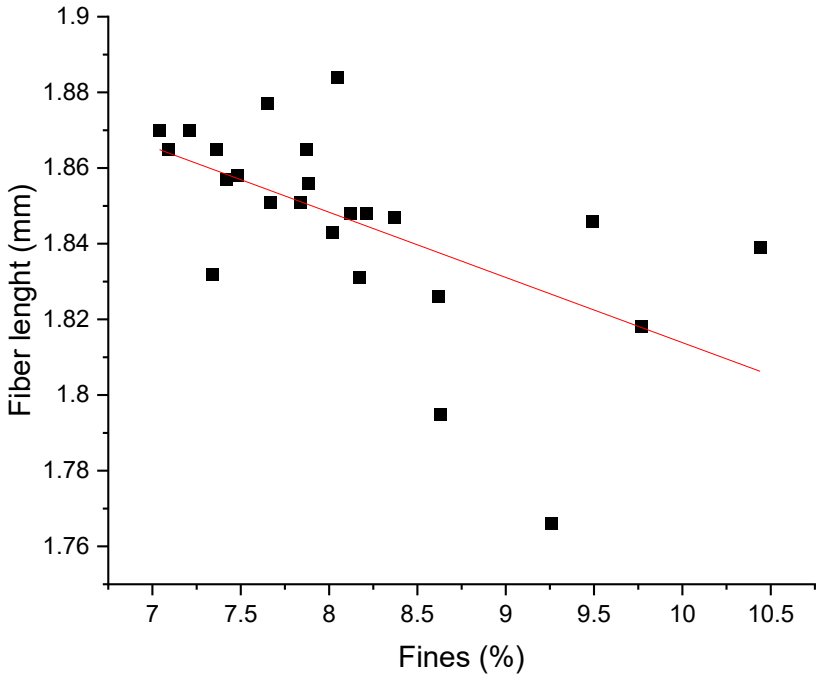

Figure 13. Dependency between fine contents and of fiber length. Red line presents a line fitting of data plots.

5.1.2 The influence of mixing on DES pretreatment

Mechanical treatments are shown to cause deformations on fibers even though they do not cause loss of strength to individual fibers. (Joutsimo et al. 2005). According to

Joutsimo & Robertsen (2004), mechanical treatment of cellulose fibers causes ultra-structural changes on the fiber walls, micropore closure and macropore opening. They observed that uptake of dextran in cellulose pores was lower for samples treated with mixing and suggested that this might be due to decrease in pore volume or change of accessibility in the fiber wall pore structure. This mechanism may also prevent DES accessing the fiber pore structure and decrease swelling of mixed pulps.

The fiber properties of pulps treated with DES in the presence and absence of mixing were compared and the results are presented in Table 4. For all pulps treated without mixing the degree of fiber swelling was higher (2.23% on average). The greatest increase in swelling was observed for pulp treated with 1:1:10 (3.28%) and smallest for 1:0.5:0 (0.40%). However, the fiber lengths decreased, 2.61% on average. Curliness of fibers increased remarkably for pulps treated without mixing, 21.83% on average. Kinks (1/m) and king angles (deg) were also increased without mixing, 12.66 and 11.81% respectively. Similar to mixed samples, the content of fines correlated only with fiber length. Increased kinks and curls might be the reason for decreased fiber lengths as remarkable increase in fines content was not observed.

Table 3. The effect of mixing on fiber properties, i.e. fiber properties of samples treated in refWater, DESs with no added water and water to CC ratio of 10 with and without mixing (marked with *) during the treatment.

Sample name	Fiber width (µm)	Fiber lenght (mm)	Curl (%)	Kink (1/m)	Kink angle (deg)	Fines (%)
1:2:0	36.81	1.818	15.49	4060	31.09	9.77
1:2:0*	37.90	1.802	19.93	4483	35.04	8.91
1:2:10	36.99	1.865	16.26	3999	31.39	7.87
1:2:10*	38.11	1.784	21.1	4730	36.42	9.38
1:1:0	37.20	1.846	16.33	4193	31.63	9.49
1:1:0*	37.94	1.831	19.47	4475	34.94	8.32
1:1:10	36.88	1.865	16.32	4115	31.74	7.36
1:1:10*	38.09	1.791	20.7	4698	36.07	10.67
1:0.5:0	37.56	1.858	16.39	3916	32.55	7.48
1:0.5:0*	37.71	1.827	18.43	4421	34.15	7.68
1:0.5:10	37.12	1.851	17.36	4154	32.62	7.67
1:0.5:10*	37.74	1.773	20.95	4777	36.68	10.60
refWater	37.00	1.795	18.34	4398	32.83	8.63
refWater*	37.86	1.763	21.13	4880	36.94	10.05

5.1.3 FTIR

According to Zhu et al. (2021), three cellulose hydrogen bonding peaks for O(2)H…O(6), O(3)H…O(5) and O(6)H….O(3') can be detected and fitted to OH stretching area of FTIR spectra. Measured OH-stretching area bands had clearly differing shapes as shown in Figure 13 and 14. RefUrea treated pulp had the widest characteristics peaks. Non-treated pulp had more narrow peak shape and especially the pulp with the highest degree of swelling (treated with 1:0.5:0) had wider peak shapes which seemed promising for hydrogen bond analysis.

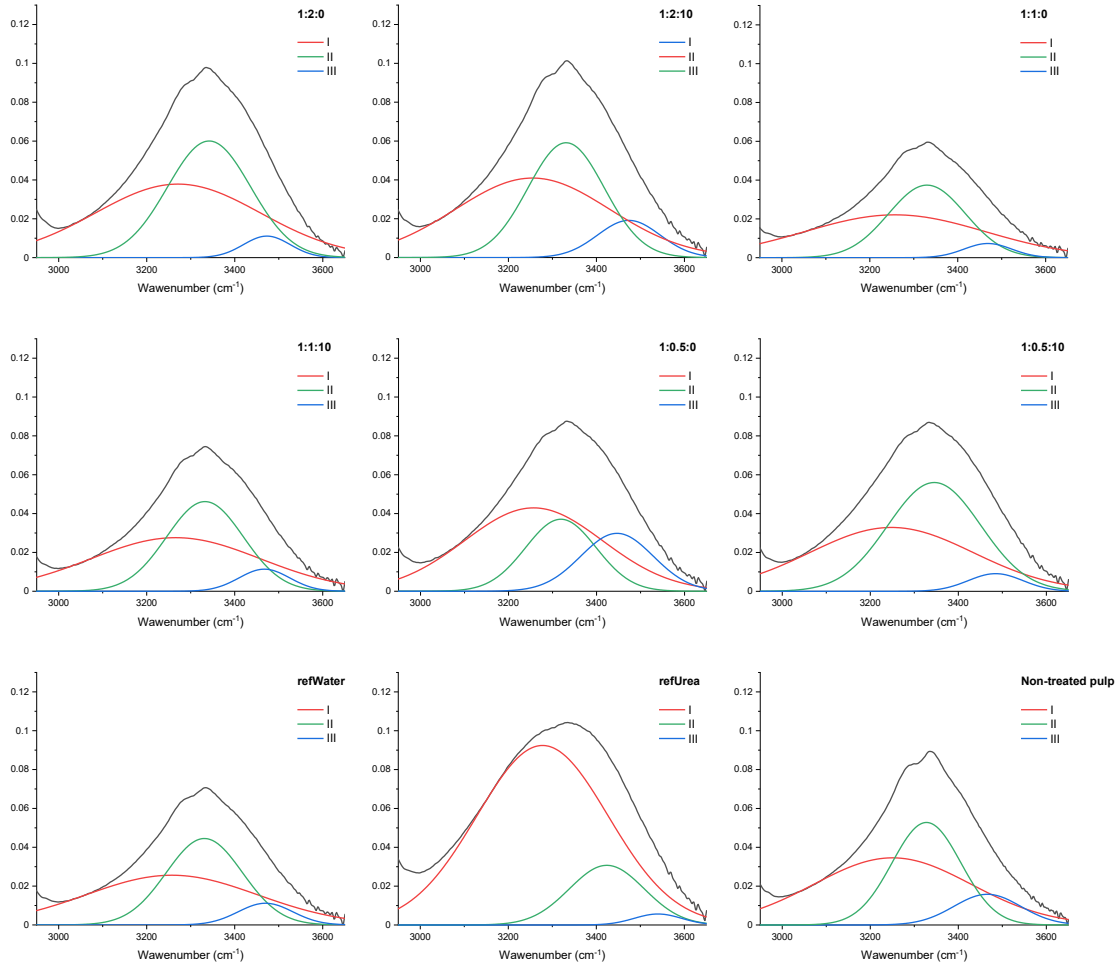

Figure 14. FTIR peak fittings for some DES treated samples and references. Raw data is the black curve and colored fittings describe following intramolecular hydrogen-bonds: I O(6)H…O(3'), II O(3)H...O(5), III O(2)H...O(6).

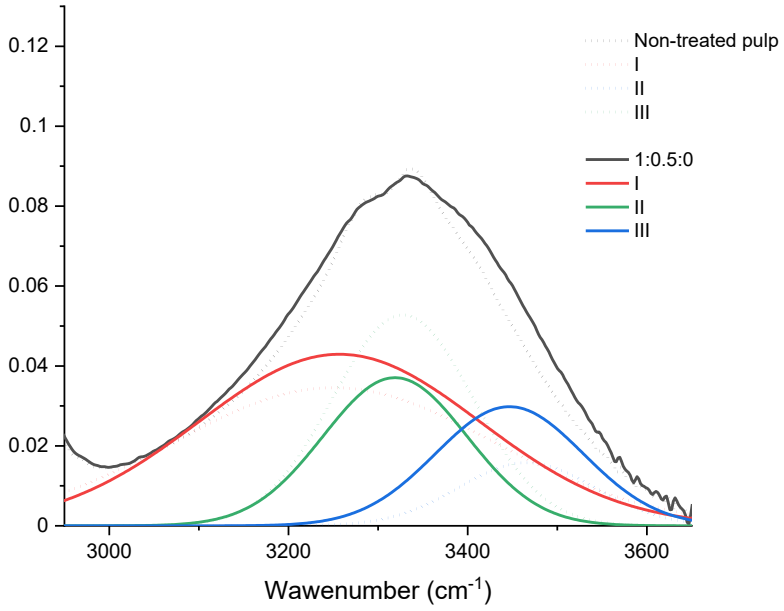

Figure 15. FTIR peak fittings for non-treated pulp compared swollen pulp treated with DES 1:0.5:0. I is O(6)H…O(3'), II O(3)H...O(5) and III O(2)H...O(6).

For non-treated pulp the O(6)H...O(3') content was calculated to be 53.68%, while DES treated pulps had contents from 44.97 to 55.77%. There was no clear trends in O(6)H...O(3') contents as function of water content in DESs, neither did the untreated pulp deviate from treated ones as seen in Figure 15. Only exception was refUrea, which had clearly the largest content of O(6)H...O(3').

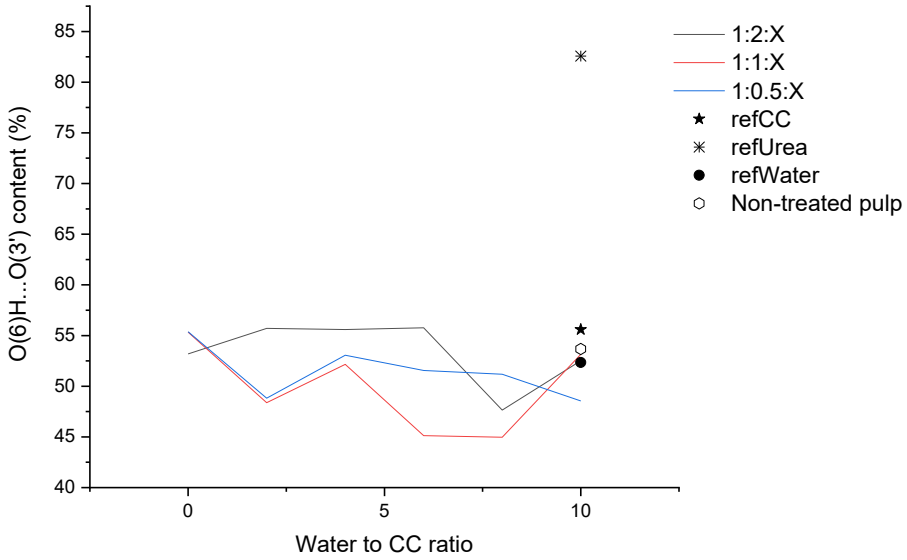

Figure 16. O(6)H...O(3') content as a function of water content.

No clear trends could be observed from O(3)H...O(5) data either as illustrated in Figure 16. RefUrea and 1:0.5:0 pulps had clearly lower contents but otherwise no remarkable variance was observed.

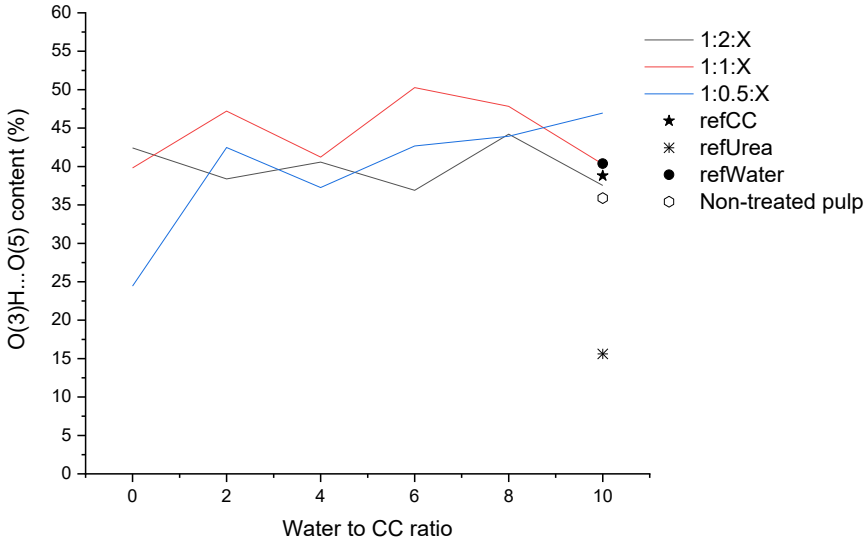

Figure 17. O(3)H...O(5) content as a function of DES water content.

Considering O(2)H...O(6) bond contents, 1:0.5:X DESs had a decreasing trend in content with increasing water content (Figure 17). However, 1:2:X DESs had the opposite trend. Non-treated pulp seemed to have a higher O(2)H...O(6) content than DESs and references except for 1:0.5.X, which had clearly higher contents with smaller water amounts.

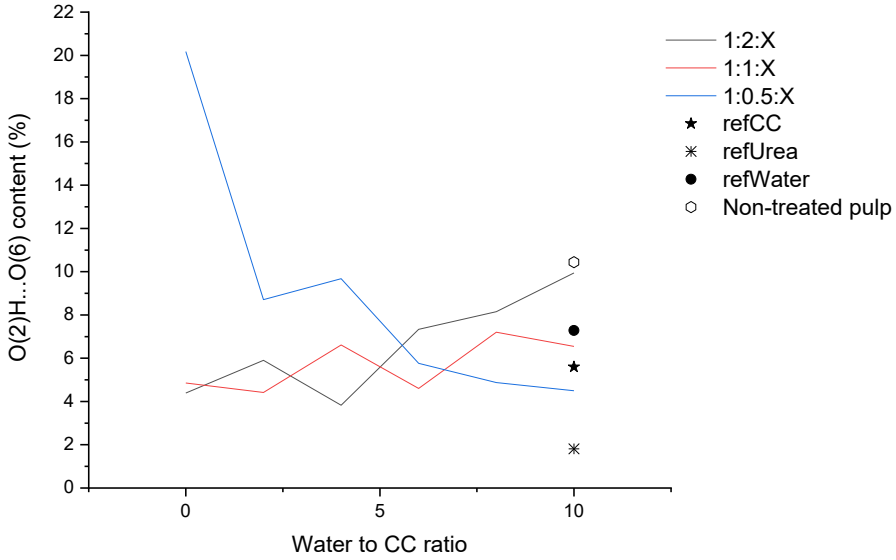

Figure 18. O(2)H...O(6) content as a function of DES water content.

Bond lengths or bond energies were calculated with Equations 10 and 11 and are presented in Tables 5 and 6. Results did not show any trends either but the values for all pulps were relatively same. Hydrogen bond contents, content relations, peak positions, energies, nor lengths correlated with fiber widths even though it was expected as the increase in fiber width is supposed to be caused by breakage of hydrogen bonds. The differences between area of O(2)H...O(6) ja O(3)H...O(5) was around 10% on average. However, for the pulp with the highest degree of swelling (treated with 1:0.5:0) the difference was 31% which indicates that some changes in the hydrogen bond network have occurred.

Table 4. H-bond peaks, bond energies and lengths of DES treated and reference pulps. Numbers describe the following bonds: I O(6)H…O(3'), II O(3)H...O(5) and III O(2)H...O(6).

Sample name	H-bond	Wawenumber (cm^{-1})	Area volume (%)	Bond energy (kJ/mol)	Bond lenght (ÅÅ)
1:2:0	I	3270.84	53.19	1.550	2.756
	II	3341.74	42.42	1.261	2.772
	III	3472.86	4.39	0.724	2.801
1:2:2	I	3246.04	55.71	1.652	2.750
	II	3329.41	38.39	1.311	2.769
	III	3463.63	5.90	0.762	2.799
1:2:4	I	3269.01	55.60	1.558	2.755
	II	3339.75	40.57	1.269	2.771
	III	3477.04	3.83	0.707	2.802
1:2:2	I	3265.99	55.77	1.570	2.755
	II	3329.46	36.90	1.311	2.769
	III	3465.75	7.33	0.753	2.800
1:2:8	I	3234.92	47.65	1.697	2.748
	II	3337.83	44.20	1.277	2.771
	III	3490.46	8.15	0.652	2.805
1:2:10	I	3254.8	52.52	1.616	2.752
	II	3331.21	37.53	1.304	2.769
	III	3473.73	9.94	0.721	2.802
1:1:0	I	3257.33	55.34	1.606	2.753
	II	3330.07	39.81	1.308	2.769
	III	3468.62	4.85	0.742	2.800
1:1:2	I	3249.68	48.37	1.637	2.751
	II	3342.89	47.21	1.256	2.772
	III	3475.65	4.42	0.713	2.802
1:1:4	I	3253.84	52.16	1.620	2.752
	II	3336.41	41.23	1.282	2.771
	III	3474.81	6.61	0.716	2.802
1:1:6	I	3238.73	45.12	1.682	2.748
	II	3344.42	50.28	1.250	2.772
	III	3495.34	4.60	0.632	2.806
1:1:8	I	3228.79	44.97	1.722	2.746
	II	3340.16	47.83	1.267	2.771
	III	3467.24	7.20	0.747	2.800
1:1:10	I	3265.77	53.15	1.571	2.755
	II	3332.51	40.30	1.298	2.770
	III	3467.39	6.54	0.747	2.800
1:0.5:0	I	3256.87	55.38	1.608	2.753
	II	3318.9	24.44	1.354	2.767
	III	3446.5	20.18	0.832	2.795
1:0.5:2	I	3254.07	48.82	1.619	2.752
	II	3335.55	42.48	1.286	2.770
	III	3456.13	8.71	0.793	2.798

Table 5. H-bond peaks, bond energies and lengths of DES treated and reference pulps. Numbers describe the following bonds: I O(6)H…O(3'), II O(3)H...O(5) and III O(2)H...O(6).

Sample name	H-bond	Wawenumber (cm^{-1})	Area volume (%)	Bond energy (kJ/mol)	Bond lenght (ÅÅ)
1:0.5:4	I	3247.39	53.07	1.646	2.75
	II	3328.13	37.26	1.316	2.769
	III	3467.48	9.67	0.746	2.8
1:0.5:6	I	3259.02	51.56	1.599	2.753
	II	3336.18	42.68	1.283	2.77
	III	3477.82	5.76	0.704	2.802
1:0.5:8	I	3262.14	51.18	1.586	2.754
	II	3341.08	43.94	1.263	2.772
	III	3471.78	4.88	0.729	2.801
1:0.5:10	I	3248.16	48.54	1.643	2.751
	II	3345.45	46.96	1.245	2.773
	III	3484.75	4.50	0.676	2.804
refCC	I	3256.93	55.60	1.607	2.753
	II	3337.18	38.80	1.279	2.771
	III	3475.78	5.60	0.712	2.802
refUrea	I	3277.75	82.57	1.522	2.757
	II	3423.83	15.62	0.925	2.79
	III	3539.99	1.81	0.45	2.816
refWater	I	3257.06	52.34	1.607	2.753
	II	3331.07	40.38	1.304	2.769
	III	3469.99	7.28	0.736	2.801
Non-treated pulp	I	3250.51	53.68	1.634	2.751
	II	3327.7	35.89	1.318	2.769
	III	3465.97	10.44	0.753	2.8

Urea can react with cellulose in high temperature and form a carbamate bond which alters the FTIR spectra at around 1715 cm^{-1} (Sirviö et al. 2015) and 3420 cm^{-1} (Zhang et al. 2013), of which the latter is within the OH-stretching area. Wider spectra of refUrea peak around these areas can be seen in Figure 18. This was not observed on other samples, which indicates that DESs do not cause chemical alteration to cellulose fibers.

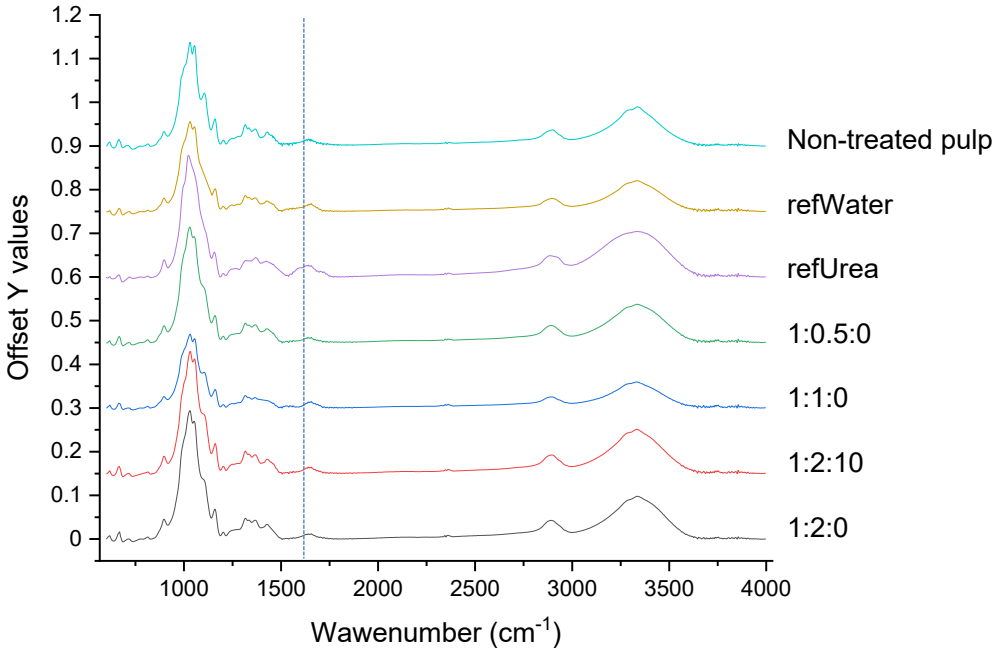

Figure 19. FTIR spectra of various pulp samples. Possible carbamate peak appears as a wider shoulder on refUrea spectra at around 1715 cm^{-1} and may also have caused alteration at around 3420 cm^{-1}.

5.1.4 Determination of acidic groups

The concentration of acidic groups of the DES-treated and TEMPO-oxidized samples is presented in Table 7. Surprisingly the pure water reference samples had the highest concentration of acidic groups, 0.46 mmol/g. Effect of water in DES samples on acid groups was not significant as the averages were 0.29 and 0.31 mmol/g for 1:0.5:0 and 1:0.5:10, respectively. The values are clearly lower than reported in literature (Sirviö et al. 2019, Saito et al. 2006). One reason for increased reactivity of water treated samples might be related to higher content of kinks and curls, which increase the accessibility to chemicals (Chandra et al. 2019). Insufficient washing procedure of the pulp before TEMPO-treatment might be a possible reason for some of the hydroxyl groups to be occupied as it was observed by Tenhunen et al. (2018) and thus inhibiting the oxidation. The number of inhibited hydroxyl groups found by Tenhunen et al. was however minor, so other factors affecting the reactivity remain to be investigated later.

Table 6. Concentration of acidic groups after TEMPO treatment for DES-pretreated samples.

Sample name	Concentration of acidic groups (mmol/g)	Average concentrations of acidic groups (mmol/g)
1:0.5:0 A	0.291	0.292
1:0.5:0 B	0.292	
1:0.5:10 A	0.308	0.308
1:0.5:10 B	0.308	
refWater A	0.458	0.457
refWater B	0.456	

5.1.5 Nanofibrillation

Nanofibrillation of DES treated pulps were made probably with too small amounts of pulp which is why new experiments would be needed to analyze if aqueous DESs can be used to nanofibrillation. However, the pulps did not clog in the homogenizer which is promising. For future research it would be interesting to test if refWater treated pulp can be used to produce nanofibrillated cellulose.

5.2 DES properties

DESs prepared for analysis were stored in closed glass bottles at room temperature. Red crystals were observed to be precipitated in DES solutions after they were settling for one week. Some samples had very thin, white flakes floating on the liquid surface, which were likely precipitated choline chloride.

5.2.1 Viscosity

DES viscosities were measured at 20 and 100 °C with shear rates from 0.1 s^{-1} to 10 s^{-1}. Viscosities varied from 87.34 to 135.51 Pa.s with shear rate of 0.1s^{-1} and in 100 °C from 1.16 to 1.71 Pa.s. Values for all samples are presented in Appendix 3. The viscosities of the DES samples decreased drastically as a function of shear rate and temperature. Non-Newtonian behavior at 20 °C was in line with literature (Kadom & Abdullah 2016, Mjalli & Ahmed 2016).

Viscosity dependency on shear rate can clearly be seen in Figure 19. However, increasing water content did not have a decreasing monotonic trend on the viscosity, controversary

to literature (Kadhom & Abdullah 2016, Gygli et al. 2020, Du et al. 2016) and to visual examination. Direct comparison of viscosities to those reported in the literature was impossible due to lack of information about shear rates (Xie et al. 2014, Shah & Mjalli 2014). The viscosities with minimum shear rates increased for all samples until CC:water ratio of 1:4, then decreased and increased again until CC:water ratio of 1:10, see Figure 20. With the higher shear rate the differences in viscosities were negligible which can be seen in Figure 21.

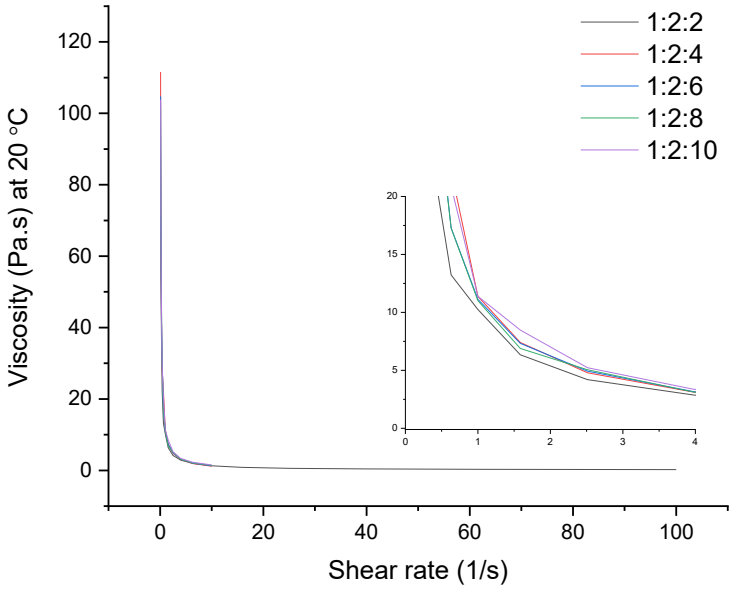

Figure 20. DES viscosities as a function of shear rate at 20 °C, insert picture is magnified from 0 to 20 Pa.s.

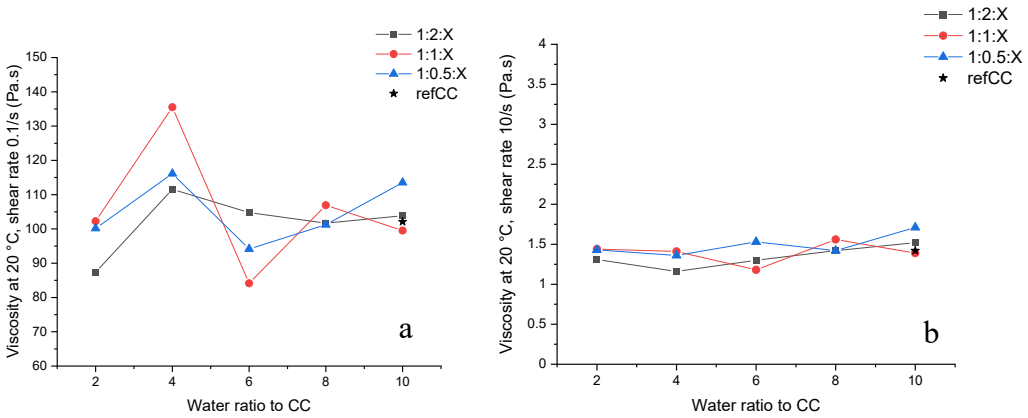

Figure 21. DES viscosities as a function of water content at 20 °C with shear rates of a) 0.1/s and b) 10/s.

Viscosities were measured with same parameters at 100 °C but it should be noted that the possible boiling of water during the measurements might have had an effect on the results.

Especially with low shear rates, anomalies were observed in the viscosities as shown in Figure 21 with few examples. These results should be interpreted with caution.

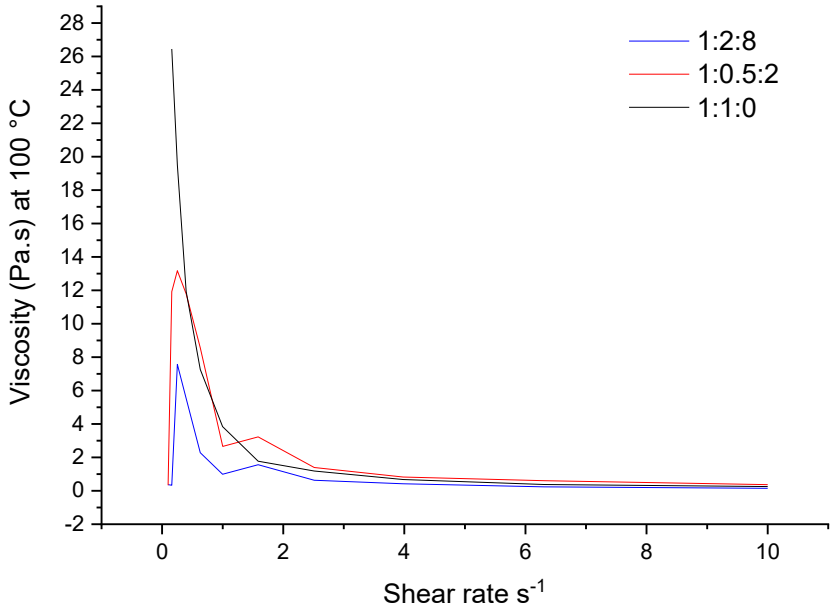

Figure 22. Viscosities of DESs 1:2:8, 1:0.2:2 and 1:1:0 at 100 °C as a function of shear rate.

In accordance with literature (Kadom & Abdullah 2016, Mjalli & Ahmed 2016), DES viscosities were clearly lower at higher temperatures. Viscosity varied from 73.00 to 0.33 Pa.s with shear rate of 0.1 s^{-1} and from 0.37 to 0.13 Pa.s with shear rate of 10 s^{-1}. RefCC had remarkably higher viscosity at 100 °C (304.14 Pa.s) with shear rate of 0.1 s^{-1}. European Chemicals Agency (2013) reported that CC:water mixture should behave as a Newtonian fluid in 75% aqueous solution even at temperatures under 40 °C with shear rates between 10 to 200 s^{-1}. They reported the viscosity of the mixture to be 0.014 Pa.s at 40 °C, which is somewhat comparable to 0.77 Pa.s obtained in this work at 100 °C with 10 s^{-1}. Viscosities did not seem to exhibit ideal Newtonian behavior in high temperatures, but the viscosity decreased with increasing shear rate as presented in Figure 22.

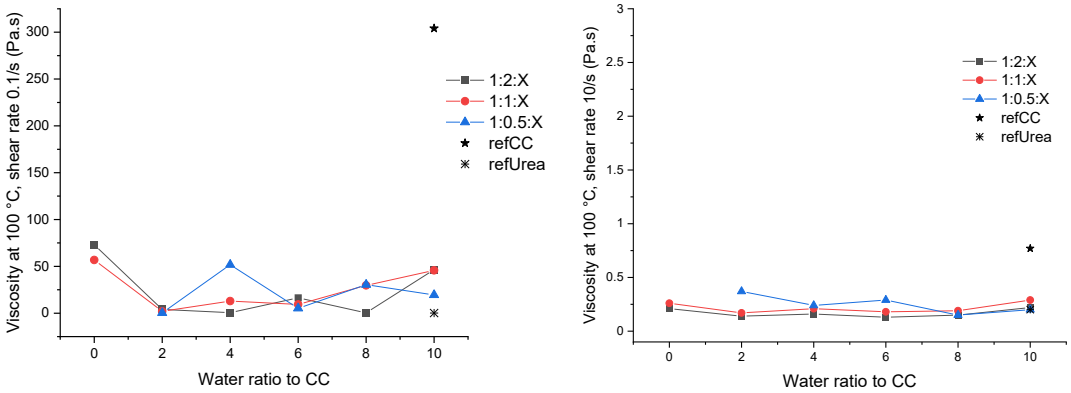

Figure 23. DES viscosities at 100 °C with shear rates of 0.1/s and 10/s.

5.2.2 pH

All values for pH of DESs are presented in Table 8. As expected, increase in water content decreased pH in all samples. RefCC had clearly the lowest pH, 4.99. Presence of urea in aqueous solutions has been confirmed to increase pH (Bull et al. 1964) and even when there are less molecules of urea than CC it seems to have a greater effect on pH. Di Pietro et al. (2021) stated that when CC:U DES is diluted with water the hydroxyl protons of choline became completely hydrated when water concentration exceeds 33 wt.%. Basic pH is in accordance to Sculcova et al. (2018) conclusion about HBD component mainly determining the pH of DES. Overall weaker hydrogen bonds of urea in presence of water (Di Pietro et al. 2021) might also be one reason for urea-weighted pH values. RefUrea did not have the highest pH but that is probably a result from higher measurement temperature as it is known to decrease pH for DESs (Hayyan et al. 2012, Sculcova et al. 2018).

Table 7. DES pHs in 23 °C. Literature references: [1] Shah & Mjalli 2014 [2] Morais et al. 2018.

Sample name	Water (wt.%)	pH	Water (w-%) [2]	pH [2]
1:2:0	0	10.97	0	10.07 [1] 9.78
1:2:2	12	10.05	16.7	9.12
1:2:4	22	9.96	20.0	8.94
1:2:2	29	9.95	25.0	8.9
1:2:8	36	9.86	33.3	8.86
1:2:10	41	9.8	50.0	8.3
1:1:0	0	-	0	10.4
1:1:2	15	10.1	16.7	9.91
1:1:4	26	9.83	20.0	9.77
1:1:6	35	9.73	25.0	9.56
1:1:8	42	9.93	33.3	9.05
1:1:10	47	9.64	50.0	8.94
1:0.5:0	0	-	0	10.58
1:0.5:2	18	10.25	16.7	10.18
1:0.5:4	30	9.82	20.0	10.01
1:0.5:6	39	9.75	25.0	9.87
1:0.5:8	46	9.63	33.3	9.71
1:0.5:10	51	9.56	50.0	9.63
refCC	20	4.99	-	-
refUrea (50 °C)	37	9.27	-	-

The pHs measured in this work had similar trends than reported earlier in the literature (Morais et al. 2018) as illustrated in Figure 23. The largest deviation was observed in DESs 1:2:x which had clearly higher pHs than repoted in Morais et al. measurements.

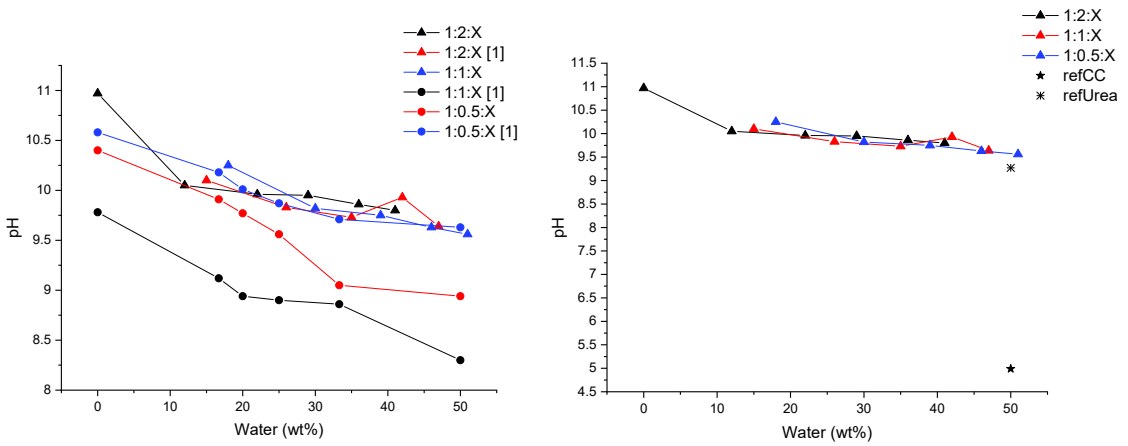

Figure 24. DES pHs at 23 °C, left with references from literature without refUrea and refCC and right scaled for refCC. Reference points from [1] Morais et al. 2018.

5.2.3 Conductivity

Conductivity of all DESs increased monotonically with increasing water content as presented in Figure 24. Conductivity of 1:2:0, 0.37 mS/cm, was a bit higher than reported in literature (0.199 mS/cm, Abbott et al. 2006) which is probably caused by absorbed water in 1:2:0. All conductivity results are presented in Table 9. Increase in conductivity was expected as water increases the fluidity of the DES thus allowing movement of charge carriers (Du et al. 2016) even though ion concentration decreases with addition of water. Remarkable increase of conductivity would allow usage of aqueous CC:U in electrochemical processes.

Table 8. DES conductivities. Literature reference [1] Abbott et al. 2006, in 40 °C.

Sample name	conductivity	literature [1]
1:2:0	0.37	0.199
1:2:2	8.23	
1:2:4	28.21	
1:2:2	39.38	
1:2:8	53.23	
1:2:10	62.36	
1:1:0	-	
1:1:2	15.17	
1:1:4	33.65	
1:1:6	57.55	
1:1:8	64.08	
1:1:10	77.48	
1:0.5:0	-	
1:0.5:2	18.28	
1:0.5:4	44.45	
1:0.5:6	65.79	
1:0.5:8	78.47	
1:0.5:10	85.69	
refCC	20.42	
refUrea (53 °C)	0.64	

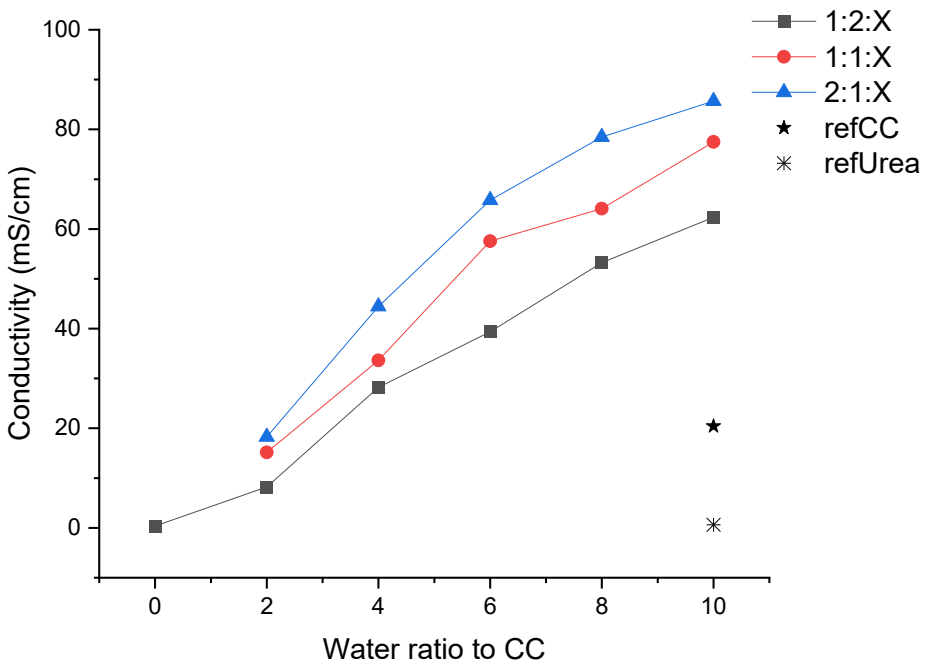

Figure 25. Conductivity as a function of increasing water content in DESs.

5.2.4 Kamlet-Taft parameters

Solvatochromic method

Spectral data from Nile red in water and cyclohexane diverged from other solvents as presented in Figure 25. The absorption curve with low intensity of water is probably caused by poor solubility of Nile red in water. Large dipole moment of Nile red is stabilized with increasing local polarity which causes bathochromic shift (Swain & Mishra 2016). This is clearly seen in Figure 26 as polar solvents have caused a clear bathochromic shift compared to non-polar cyclohexane.

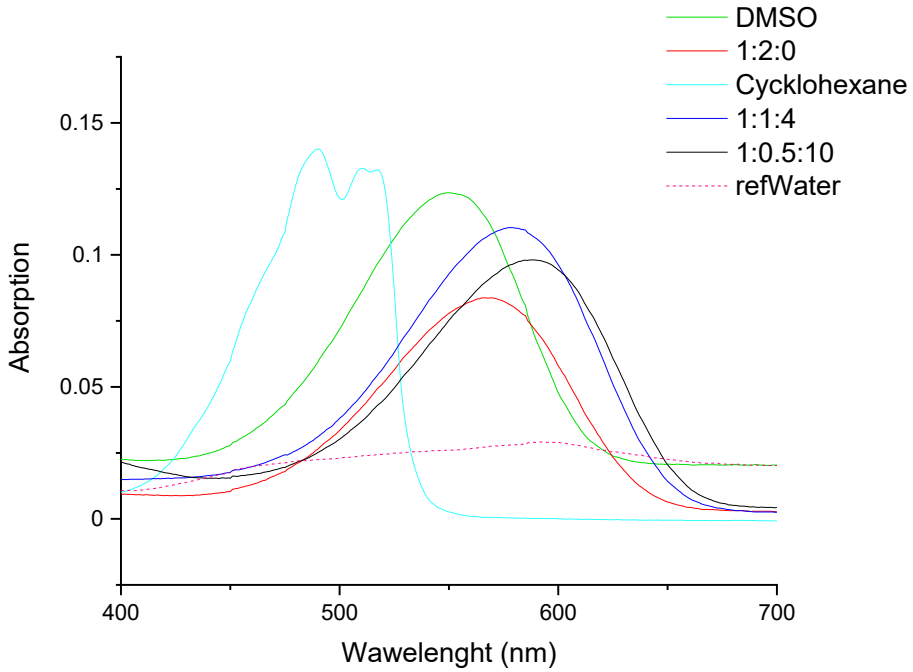

Figure 26. Absorption spectra of Nile red in different solvents.

Clear bathochromical shift was observed in Nile red with increasing water content of the DESs, Figure 27. Shift to longer wavelengths was found also with DENA with increasing water content as seen in Figure 28. In DESs with molar ratio of 1:0.5, 4NA had a slightly hypsochromic shift when water content was increased but with other molar ratios no clear trend was observed.

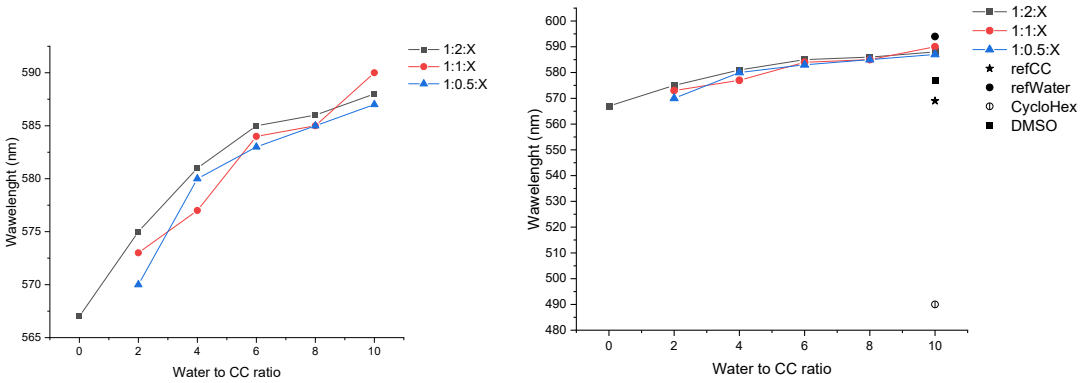

Figure 27. Absorption peaks of Nile red in DESs and reference solvents as a function of increasing water content.

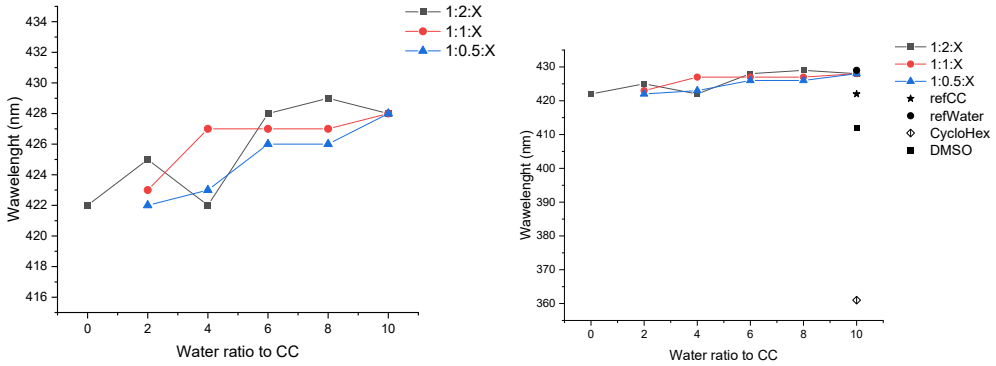

Figure 28. A bsorption peaks of N,N-diethyl-4-nitroaniline a DESs and reference solvents as a function of increasing water content.

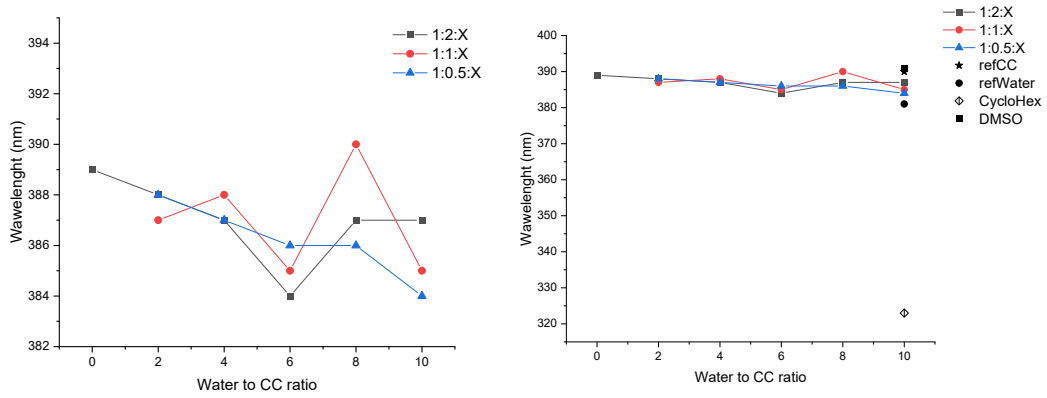

Figure 29. Absorption peaks of 4-nitroaniline in DESs and reference solvents as a function of increasing water content.

Measured wavelengths corresponding to maximum absorption of the probe can be found in Appendix 2. The solvatochromic parameters were calculated with these wavelengths

first by using DMSO and cyclohexane values and Equations 2-4 and then with ready-normalized Equations 5-7.

π* parameter

Solvent π* values increased with increasing water content with both solvent-normalized and ready-normalized methods which can be seen in Figure 29. Pure water reference and samples 1:2:8 had the highest dipolarity. The lowest values were for refCC, 1:2:0, 1:2:4 and 1:0.5:2. Values are presented in Table 10 with references obtained from the literature. The polarity increase stabilized for all DESs when the water to CC ratio exceeded 6.

There was no big difference between solvent-normalized (Eq. 2) and ready-normalized (Eq. 5) values, but Equation 5 gave systematically a slightly larger values, +0.03 on average. RefWater and DMSO values were in the π* range from literature. DES 1:2:0 π* was close to value reported by Florindo et al.'s (2018) but it differed greatly from Ren et al.'s (2016) result. The difference might result from that Ren et al. used 4NA instead of DENA to determine π*. Cai et al. (2019) had also determined π* for aqueous CC:U DES with 1% more water than used in DES 1:2:2 and the result was very close to one determined in this work. RefCC π* differed from Asares (2018) result even though same probes and ready-normalized equation had been used.

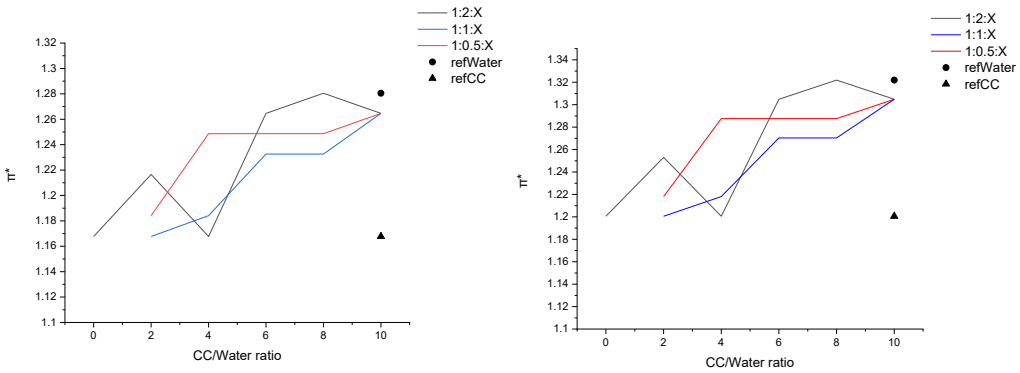

Figure 30. DES π* values as function of water content. On the left solvent-normalized (Eq. 2) values and on the right ready-normalized (Eq. 5).

Table 9. π* values for DESs and reference solvents calculated with Equations 2 and 5. Literature references are from: [1] Buhvestov et al. 1998 [2] Florindo et al. 2018 [3] Hu et al. 2014 [4] Kamlet et al. 1983 [5] Asare, S. 2018 [6] Ren et al. 2016 [7]* Cai et al. 2019, 30 wt.% water

Sample name	π* (Eq. 2)	π* (Eq. 5)	Difference	literature
1:2:0	1.17	1.20	0.03	1.14[2] 0.32[6]
1:2:2	1.22	1.25	0.04	1.24[7]*
1:2:4	1.17	1.20	0.03	
1:2:6	1.26	1.30	0.04	
1:2:8	1.28	1.32	0.04	
1:2:10	1.26	1.30	0.04	
1:1:0	-	-	-	
1:1:2	1.18	1.22	0.03	
1:1:4	1.25	1.29	0.04	
1:1:6	1.25	1.29	0.04	
1:1:8	1.25	1.29	0.04	
1:1:10	1.26	1.30	0.04	
1:0.5:0	-	-	-	
1:0.5:2	1.17	1.20	0.03	
1:0.5:4	1.18	1.22	0.03	
1:0.5:6	1.23	1.27	0.04	
1:0.5:8	1.23	1.27	0.04	
1:0.5:10	1.26	1.30	0.04	
refCC	1.17	1.20	0.03	0.72[5]
refWater	1.28	1.32	0.04	1.14[1], 1.36[3] 1.09[4]
CycloHex	0.00	-0.06	-0.06	0[5]
DMSO	1.00	1.02	0.02	1.01[3] 1.00[4]

β parameters

Solvent β-parameters were calculated with Equations 3 and 6 and are presented in Table 11. Again, it was noted that ready-normalized equations resulted in higher values, + 0.11 on average. β-parameter decreased by increasing water content as illustrated in Figure 30. Same effect is observed also with other solvents (Buhvestov et al. 1998, Hauru et al. 2012). Water reference had clearly the lowest value and CC reference the highest. This can be easily explained as choline chloride is a HBA component. Water is an amphiprotic molecule which might explain the variance in literature in addition to differences in

calculation methods and probes. However, results from this work are mainly in line with literature. The largest deviation from literature was again with results reported by Ren et al. which might be due to different equation used.

Table 10. β-values calculated with Equations 3 and 6. Literature references are from: [1] Buhvestov et al. 1998 [2] Florindo et al. 2018 [3] Hu et al. 2014 [4] Kamlet et al. 1983 [5] Asare, S. 2018 [6] Ren et al. 2016 [7]* Cai et al. 2019, 30 wt.% water.

Sample	β (Eq. 3)	β (Eq. 6)	Difference	literature
1:2:0	0.49	0.58	0.10	0.50[2], 0.82[6]
1:2:2	0.39	0.50	0.10	1.24[7]*
1:2:4	0.43	0.53	0.10	
1:2:6	0.23	0.34	0.12	
1:2:8	0.28	0.40	0.11	
1:2:10	0.30	0.42	0.11	
1:1:2	0.41	0.51	0.10	
1:1:4	0.35	0.46	0.11	
1:1:6	0.27	0.39	0.11	
1:1:8	0.40	0.51	0.10	
1:1:10	0.25	0.37	0.11	
1:0.5:2	0.46	0.56	0.10	
1:0.5:4	0.41	0.51	0.10	
1:0.5:6	0.32	0.43	0.11	
1:0.5:8	0.32	0.43	0.11	
1:0.5:10	0.23	0.34	0.12	
refCC	0.51	0.60	0.09	0.41[5]
refWater	0.13	0.25	0.13	0.49[1] 0.14[3] 0.18[4]
CycloHex	0.00	0.11	0.11	0[5]
DMSO	0.76	0.83	0.07	0.72[3] 0.76[4]

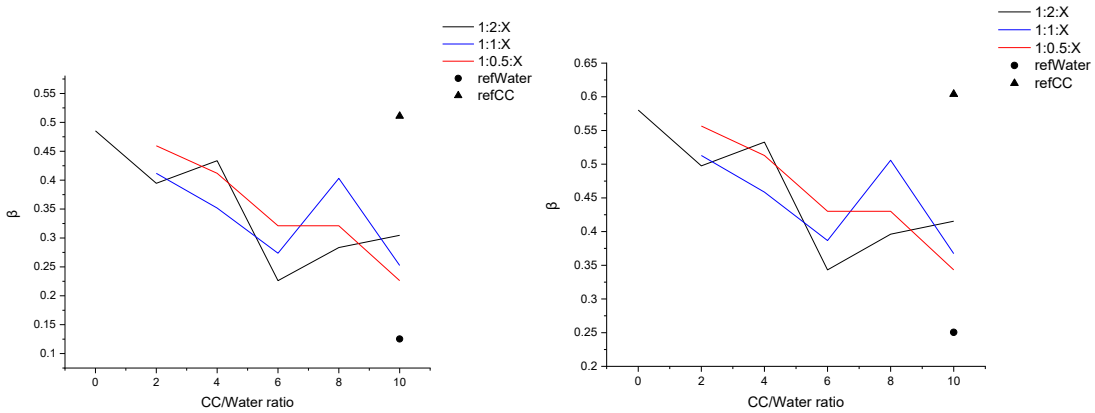

Figure 31. DES β-values as a function of water content, On the left solvent-normalized (Eq. 3) values and on the right ready-normalized (Eq. 6).

Trends with increasing water content are opposite with ready-normalized and solvent-normalized methods for α as seen in Table 12. The difference might due to using only two solvent for determination of reference line and from using Nile red instead of Reichardt's dye. The solvent-based comparison gave a decreasing reference line, opposite to Eyckens et al. example. It seems that DENA and Nile red can't be used with solvent-normalized method as the obtained parameter values do not match with literature. These deviations might also be attributed with the measurement errors. For further studies, it is suggested to test solvent-based determination of α with Nile Red and DENA with at least 5 reference solvents. Difference from ready-normalized equation values increased with increasing water content, which could indicate that solvent dipolarity affects the results more than hydrogen bond accepting ability. It is also possible that in complex cation-anion-water systems dye can preferentially interact with one of the components or clusters may form (Hauru et al. 2012). Nile red can also form clusters in aqueous solvents (Ray et al. 2019).

The α values increased distinctly with solvent-normalized method with increasing water content as illustrated in Figure 31. Pure water reference had the highest value which was also closer to literature. DES 1:2:0 α deviated remarkably from Florindo et al.'s result even with ready-normalized equation which probably results from different probe and calculation method used. Results of Cheong and Carr (1988) suggest that α should increase with increasing water content. Hauru et al. (2012) noted that the solvent α values did not change remarkably with changing water content. Thus, the values calculated with ready-normalized equation might be more reliable. However, ready-normalized equation gives drastically incorrect value for DMSO. Molecular solvents have different solvatochromic behavior compared to ionic liquid-type solvents (Xue et al. 2016) which might be the reason why DMSO value deviates so much from th evalue reported in the literature.

Table 11. α -values calculated with Equations 4 and 7. Literature references are from: [1] Buhvestov et al. 1998 [2] Florindo et al. 2018 [3] Hu et al. 2014 [4] Kamlet et al. 1983 [5] Asare, S. 2018 [6] Ren et al. 2016 [7]* Cai et al. 2019, 30 wt.% water.

Sample	α (Eq. 4)	α (Eq. 7)	Difference	Literature
1:2:0	0.61	0.68	0.07	1.42 [2]
1:2:2	0.54	0.80	0.26	2.25 [7]*
1:2:4	0.30	0.95	0.65	
1:2:6	0.43	0.95	0.52	
1:2:8	0.45	0.96	0.51	
1:2:10	0.37	1.01	0.64	
1:1:0	-	-	-	
1:1:2	0.51	0.79	0.28	
1:1:4	0.57	0.82	0.25	
1:1:6	0.42	0.95	0.53	
1:1:8	0.39	0.97	0.58	
1:1:10	0.32	1.05	0.73	
1:0.5:0	-	-	-	
1:0.5:2	0.54	0.74	0.20	
1:0.5:4	0.36	0.92	0.56	
1:0.5:6	0.40	0.94	0.54	
1:0.5:8	0.36	0.98	0.62	
1:0.5:10	0.39	0.99	0.60	
refCC	0.57	0.72	0.15	0.94 [5]
refWater	0.36	1.11	0.75	1.17 [4] 1.23 [1]
CycloHex	0.00	-0.24	-0.24	0 [4]
DMSO	0.00	0.99	0.99	0.15 [3] 0 [4]

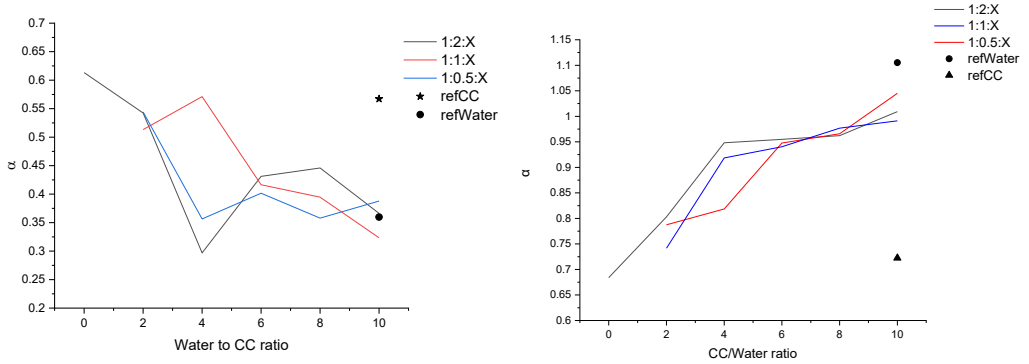

Figure 32. α -values. On the left solvent-normalized (Eq. 4) values and on the right ready-normalized (Eq. 7).

Based on obtained results and comparison to literature, it is suggested that solvent-normalized method should be used to determine π* and β and ready-normalized method for α. However, Kamlet-Taft parameters do not seem to be the best alternative to characterize DESs as the different methods and probes seem to affect the values so much that even some traditional solvents have notably different values to those reported in the literature. Parameters obtained from this work should be used only as suggestive.

Solvatomagnetic method

Both α and β -values of DESs increased with water content as seen in Table 13. Increase of β with increasing water content in contradiction with literature as previously mentioned (Buhvestov et al. 1998, Hauru et al. 2012). Because DMSO and cyclohexane were not measured, comparison to literature was more difficult than with solvatochromic method. However, based on refWater and 1:2:0, the values can be taken as directional information for other than aqueous DESs. DESs with no added water were also measured at 100 ° C but 1:0.5:0 was not liquid even at this temperature, so it was not measured at all. For 1:2:0 measurements could be made in both temperatures and it was observed that both α and β decrease with increasing temperature. Interestingly, refCC values were now closer to results of Asare (2018).

Table 12. Kamlet-Taft parameters with solvatomagnetic method. Values with [100] are measured in 100 °C. Literature references are from: [1] Buhvestov et al. 1998 [2] Florindo et al. 2018 [3] Hu et al. 2014 [4] Kamlet et al. 1983 [5] Asare, S. 2018 [6] Ren et al. 2016 [7]* Cai et al. 2019, 30 wt.% water

Sample	β	literature	α_{24}	literature
1:2:0	0.56, 0.49[100]	0.50[2], 0.82[6]	0.84, 0.74[100]	1.42[2]
1:2:2	0.50	1.24[7]*	1.00	2.25[7]*
1:2:4	0.59		1.10	
1:2:6	0.50		1.16	
1:2:8	0.69		1.23	
1:2:10	0.77		1.20	
1:1:0	0.51[100]		0.70[100]	
1:1:2	0.51		1.00	
1:1:4	0.44		1.12	
1:1:6	0.66		1.18	
1:1:8	0.61		1.23	
1:1:10	0.81		1.25	
1:0.5:0	-		-	
1:0.5:2	0.56		1.00	
1:0.5:4	0.51		1.11	
1:0.5:6	0.71		1.19	
1:0.5:8	0.77		1.24	
1:0.5:10	0.82		1.27	
refCC	0.43	0.41[5]	0.99	0.94[5]
refWater	0.44	0.49[1] 0.14[3] 0.18[4]	1.37	1.17[4] 1.23[1]

Solvatomagnetic method resulted in continuously higher values than solvatochromic method, of which the better options were chosen for comparison (solvent-normalized for β and ready-normalized for α) as presented in Table 14. The difference increased with increasing water content but as the solvatochromic parameters are only indicative, they can not be used to define the validity of solvatomagnetic parameters. Based on these comparisons, combination of solvatomagnetic and solvatochromic methods would be the best option to determine polarity parameters for DESs. Solvatomagnetic method should be used to determine α and solvatochromic method to determine π* and β. The solvatomagnetic method for determining α was also easier because PyO dissolved to solvents easier than Nile red.

Table 13. Comparison of β and α calculated with solvatomagnetic* and solvatochromic method.

Sample	β*	β (Eq. 3)	Difference	α*	α (Eq.7)	Difference
1:2:0	0.56	0.49	0.07	0.84	0.68	0.16
1:2:2	0.50	0.39	0.11	1.00	0.80	0.2
1:2:4	0.59	0.43	0.16	1.10	0.95	0.15
1:2:6	0.50	0.23	0.27	1.16	0.95	0.21
1:2:8	0.69	0.28	0.41	1.23	0.96	0.27
1:2:10	0.77	0.30	0.47	1.20	1.01	0.19
	-	-	-	-	-	
1:1:2	0.51	0.41	0.1	1.00	0.79	0.21
1:1:4	0.44	0.35	0.09	1.12	0.82	0.3
1:1:6	0.66	0.27	0.39	1.18	0.95	0.23
1:1:8	0.61	0.40	0.21	1.23	0.97	0.26
1:1:10	0.81	0.25	0.56	1.25	1.05	0.2
	-	-	-	-	-	
1:0.5:2	0.56	0.46	0.1	1.00	0.74	0.26
1:0.5:4	0.51	0.41	0.1	1.11	0.92	0.19
1:0.5:6	0.71	0.32	0.39	1.19	0.94	0.25
1:0.5:8	0.77	0.32	0.45	1.24	0.98	0.26
1:0.5:10	0.82	0.23	0.59	1.27	0.99	0.28
refCC	0.43	0.51	-0.08	0.99	0.72	0.27
refWater	0.44	0.13	0.31	1.37	1.11	0.26

5.2.5 Relationship of polarity parameters and fiber swelling

Polarity parameters of DESs were compared to fiber widths of DES treted samples. It was found that solvatochromic β value calculated with solvatomagnetic method had a slight correlation with fiber width as presented in Figure 32 (values based on the Equation 3). Higher β seems to lead in larger fiber width. Solvatomagnetic method derived α had also a slight correlation to fiber width as presented in Figure 32. Figure 33 presents π* (Eq. 2) as a function of fiber width. It seems that higher π* values lead to smaller fiber width. The red lines in the pictures are linear fits computed with Origin but they did not have good R^2 values which were 0.22, 0.022, 0.232 and 0.080 for π* (Eq. 2), α (solvatomagnetic), β (Eq. 3) and β-α, respectively. It is possible that the relations are not linear, which seems to be the case especially for β-α. These parameters could however be used to roughly estimate the ability of solvent to swell cellulose fibers. Hauru et al. (2017) studied cellulose dissolution and regeneration and concluded that β-α of the used solvent

correlated best with dissolution behavior. Figure 33 presentx β-α as a function of fiber width. β-α seems to have the best correlation to fiber width so that smaller difference in β and α leads to better swelling.

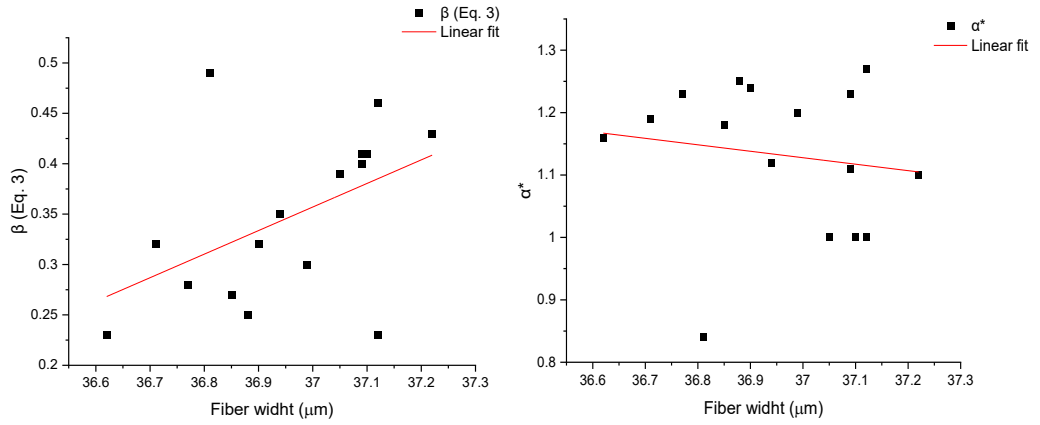

Figure 33. β (Eq. 3) and α (solvatomagnetic) as a function of fiber width.

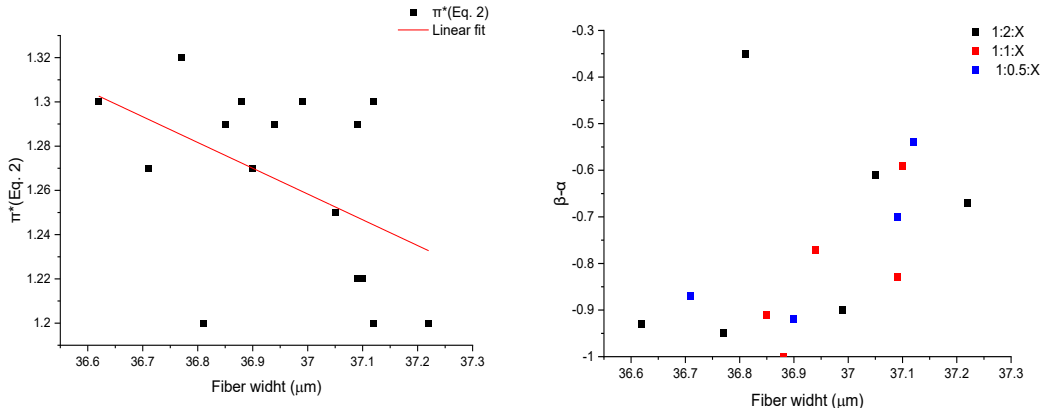

Figure 34. π* (Eq. 2) and β (Eq. 3)-α (solvatomagnetic) as a function of fiber width.

6 SUMMARY

DESs have gained attention as customizable and low-cost green solvents. CC:U is a hygroscopic mixture and it would be more practical to use it as an aqueous solvent, especially in industrial applications. In this study, Kraft cellulose pulp was treated with CC:U DESs with different molar ratios and water contents. The literature review consists of descriptions about the structure and applications for cellulose and DES, chemistry of cellulose swelling in DES treatment and the effect of water on CC:U.

In the experimental part of this work cellulose pulp was treated in CC:U DESs which had molar ratios of 1:2, 1:1 and 1:0.5 and water contents of 0, 2, 4, 6, 8 and 10, related to CC. It should be noted that the samples without any added water are, however, aqueous solutions as the DES components were not dried. Reference treatments were made in CC:water, urea:water, pure water, water (pH 10) and CC:water (pH 10). Treatments were conducted in closed bottles placed in 100 °C oil-bath with magnetic stirrer for one hour. The efficiency of treatments was analyzed by comparing the fiber properties of treated pulps. DES 1:0.5:0 treated pulp showed the largest increase in fiber width (37.12 µm) compared to non-treated pulp (36.03 µm). All DESs increased the fiber width, 1 µm on average. Interestingly also pure water caused swelling to the fiber. FTIR analysis indicated that DESs didn't cause any changes in chemical structure of cellulose. The reactivity of DES treated pulps was tested with TEMPO-treatment and surprisingly refWater treated pulp had the largest concentration of attached functional groups. Few treatments were re-made without mixing and it was found that these pulps had increased widths compared to samples made with mixing. The effect of mixing should be investigated more in-depth in future research.

Viscosity of DESs was observed to decrease remarkably with increasing temperature and shear rate. Controversary to literature and visual examination, viscosity did not seem to decrease monotonically with increasing water content. Conductivity of DESs increased drastically with increasing water content. DESs with no added water had highest pHs and decreased with increasing water content.

Polarity of solvents can be described by Kamlet-Taft parameters for dipolarity/dipolarizability, hydrogen bond acceptance and hydrogen bond donating ability. The parameters were determined with solvatochromic and solvatomagnetic

methods. In solvatochromic method, both solvent-normalized and ready-normalized methods were studied. Results were rather controversary compared to each other especially considering the effect of water. When the data was compared to literature, the best method to determine π* and β for DESs appeared to be solvatochromic method with ready-normalized equations. Instead, α should preferably be determined with solvatomagnetic method.

As an outcome of this work, water does not seem to affect too much the cellulose treatment in DES, yet it clearly had effect on DES properties. However, properties of aqueous DESs were advantageous as especially lower viscosity eases the handling of solvent. Kamlet-Taft parameters can be used to estimate the fiber swelling properties of DES but more research on the validity of the method is still needed.

REFERENCES

Abbott, A. P., Boothby, D., Capper, G., Davies, D. L., and Rasheed, R. K., 2004. Deep Eutectic Solvents Formed between Choline Chloride and Carboxylic Acids: Versatile Alternatives to Ionic Liquids. Am. Chem. Soc. 126 (29), 9142–9147.

Abbott, A. P., Capper, G., Davies, D. L., Munro, H. L., Rasheed, R. K., & Tambyrajah, V., 2001. Preparation of novel, moisture-stable, Lewis-acidic ionic liquids containing quaternary ammonium salts with functional side chains. Chemical Communications, (19), 2010-2011.

Abbott, A. P., Capper, G., Davies, D. L., Rasheed, R. K., and Tambyrajah, V., 2003. Novel solvent properties of choline chloride/urea mixtures. Chemical communications, (1), 70–7.

Alonso, D. A., Baeza, A., Chinchilla, R., Guillena, G., Pastor, I. M., and Ramón, D. J., 2016. Deep Eutectic Solvents: The Organic Reaction Medium of the Century. Eur. J. Org. Chem., 2016 (4), 612–632.

Asare, S. 2018. Synthesis, Characterization and MolecularDynamic Simulations of Aqueous CholineChloride Deep Eutectic Solvents. Thesis (PhD). South Dakota State University. Available from: https://openprairie.sdstate.edu/etd/2968

Bharimalla, A., Deshmukh, S., Patil, P.G. & Nadanathangam, V., 2015. Energy Efficient Manufacturing of Nanocellulose by Chemo- and Bio-Mechanical Processes. World Journal of Nano Science and Engineering, 5, 204-212.

Brandt, A., Gräsvik, J., Hallett, J. P., and Welton, T., 2013. Deconstruction of lignocellulosic biomass with ionic liquids. Green Chemistry, 15 (3), 550–583.

Buhvestov, U., Rived, F., Ràfols, C., Bosch, E., and Rosés, M., 1998. Solute–solvent and solvent–solvent interactions in binary solvent mixtures. Part 7. Comparison of the enhancement of the water structure in alcohol–water mixtures measured by solvatochromic indicators. Journal of Physical Organic Chemistry, 11 (3), 185–192.

Bull, H. B., Breese, K., Ferguson, G. L., and Swenson, C. A., 1964. The pH of urea solutions. Archives of Biochemistry and Biophysics, 104 (2), 297–304.

Cai, C., Li, F., Liu, L., and Tan, Z., 2019. Deep eutectic solvents used as the green media for the efficient extraction of caffeine from Chinese dark tea. Separation and Purification technology, 227, 115723.

Chandra, R., Wu, J., and Saddler, J., 2019. The Application of Fiber Quality Analysis (FQA) and Cellulose Accessibility Measurements To Better Elucidate the Impact of Fiber Curls and Kinks on the Enzymatic Hydrolysis of Fibers. ACS Sustainable Chemistry & Engineering, 7 (9).

Chen, Y., Zhang, L., Yang, Y., Pang, B., Xu, W., Duan, G., Jiang, S. and Zhang, K., 2021. Recent Progress on Nanocellulose Aerogels: Preparation, Modification, Composite Fabrication, Applications. Advanced Materials, 33 (11), 2005569.

Cheong, W. J. and Carr, P. W., 1988. Kamlet-Taft .pi.* polarizability/dipolarity of mixtures of water with various organic solvents. Analytical Chemistry, 60 (8), 820–826.

Di Pietro, M. E., Tortora, M., Bottari, C., Colombo Dugoni, G., Pivato, R. V., Rossi, B., Paolantoni, M., and Mele, A., 2021. In Competition for Water: Hydrated Choline Chloride:Urea vs Choline Acetate:Urea Deep Eutectic Solvents. ACS Sustainable Chemistry Engineering, 9 (36), 12262–12273.

Docherty, K.M., Dixon, J.K. & Kulpa Jr, C.F., 2007. Biodegradability of imidazolium and pyridinium ionic liquids by an activated sludge microbial community. Biodegradation 18, 481–493

Du, C., Zhao, B., Chen, X.-B., Birbilis, N. and Yang, H., 2016. Effect of water presence on choline chloride-2urea ionic liquid and coating platings from the hydrated ionic liquid. Scientific Reports, 6, 29225.

Dwamena, A. K. and Raynie, D. E., 2020. Solvatochromic Parameters of Deep Eutectic Solvents: Effect of Different Carboxylic Acids as Hydrogen Bond Donor. [online], 65 (2), 640–646.

Earle, M. and Seddon, K., 2002. Ionic liquids. Green solvents for the future. Pure Appl. Chem. 72, (7), 1391–1398

El Achkar, T., Fourmentin, S., and Greige-Gerges, H., 2019. Deep eutectic solvents: An overview on their interactions with water and biochemical compounds. Journal of Molecular Liquids, 288, 111028.

Eyckens, D. J., Demir, B., Walsh, T. R., Welton, T., and Henderson, L. C., 2016. Determination of Kamlet–Taft parameters for selected solvate ionic liquids. Physical Chemistry Chemical Physics, 18 (19), 13153–13157.

Fengel D., 1993. Influence of Water on the OH Valency Range in Deconvoluted FTIR Spectra of Cellulose. Wood research and technology, 47(2), 103-108.

Florindo, C., McIntosh, A. J. S., Welton, T., Branco, L. C., and Marrucho, I. M., 2018. A closer look into deep eutectic solvents: exploring intermolecular interactions using solvatochromic probes. Physical Chemistry Chemical Physics, 20 (1), 206–213.

Fotie, G., Limbo, S. and Piergiovanni, L., 2020. Manufacturing of Food Packaging Based on Nanocellulose: Current Advances and Challenges. Nanomaterials, 10 (9), 1726.

Gajardo-Parra, N. F., Cotroneo-Figueroa, V. P., Aravena, P., Vesovic, V., and Canales, R. I., 2020. Viscosity of Choline Chloride-Based Deep Eutectic Solvents: Experiments and Modeling. Journal of Chemical & Engineering Data, 65 (11), 5581–5592.

Gathergood, N., Garcia, M. T., and Scammells, P. J., 2004. Biodegradable ionic liquids: Part I. Concept, preliminary targets and evaluation. Green Chemistry, 6 (3), 166–175.

Gygli, G., Xu, X., and Pleiss, J., 2020. Meta-analysis of viscosity of aqueous deep eutectic solvents and their components. Scientific Reports, 10 (1), 1–11.

Hammond, O. S., Bowron, D. T., Edler, Karen J., Hammond, S. K. J. E., and Owron, D. T. B., 2017. Deep Eutectic Solvents Very Important Paper The Effect of Water upon Deep Eutectic Solvent Nanostructure: An Unusual Transition from Ionic Mixture to Aqueous Solution. Angew. Chem. Int. Ed., 56 (33), 9782-9785.

Hauru, L., Hummel, M., King, A., Kilpeläinen, I. & Sixta, H., 2012. Role of solvent parameters in the regeneration of cellulose from ionic liquid solutions. American Chemical Society, Biomacromolecules, 13(9), 2896-2905.

Hayyan, A., Ali Hashim, M., Mjalli, F. S., Hayyan, M., and AlNashef, I. M., 2013. A novel phosphonium-based deep eutectic catalyst for biodiesel production from industrial low grade crude palm oil. Chemical Engineering Science, 92, 81–88.

Hayyan, A., Mjalli, F. S., AlNashef, I. M., Al-Wahaibi, T., Al-Wahaibi, Y. M., and Hashim, M. A., 2012. Fruit sugar-based deep eutectic solvents and their physical properties. Thermochimica Acta, 541, 70–75.

Hayyan, M., Looi, C. Y., Hayyan, A., Wong, W. F., and Hashim, M. A., 2015. In Vitro and In Vivo Toxicity Profiling of Ammonium-Based Deep Eutectic Solvents. PLoS ONE, 10 (2), e0117934.

Heinze, T., Siebert, ., Berlin, P. & Koschella, A., 2016. Biofunctional Materials Based on Amino Cellulose Derivatives--A Nanobiotechnological Concept. Macromolecular bioscience, 16(1), 10–42.

Hu, J., Zhu, W., Yang, Q., Qian, G. & Xing, H., 2014. Solvatochromic Parameters of the Binary Mixtures of Imidazolium Chloride Ionic Liquid Plus Molecular Solvent. Applied Solution Chemistry and Modeling, 3 (4), 223-230.

Ivanova, N. V., Korolenko, E. A., Korolik, E. V., & Zhbankov, R. G., 1989. IR spectrum of cellulose. Journal of Applied Spectroscopy, 51(2), 847–851.

Joutsimo & Robertsen, 2004. The effect of mechanical treatment on softwood kraft pulp fibers. Fiber Wall. Paperi ja Puu – Paper and Timber, accepted for publication. Paperi ja Puu Oy.

Joutsimo, O., Wathén, R., and Tamminen, T., 2005. Effects of fiber deformations on pulp sheet properties and fiber strength, 87.

Juneidi, I., Hayyan, M., and Hashim, M. A., 2015. Evaluation of toxicity and biodegradability for cholinium-based deep eutectic solvents. RSC Advances, 5 (102), 83636–83647.

Jung, D., Jung, J. B., Kang, S., Li, K., Hwang, I., Jeong, J. H., Kim, H. S., and Lee, J., 2021. Toxico-metabolomics study of a deep eutectic solvent comprising choline chloride and urea suggests in vivo toxicity involving oxidative stress and ammonia stress. Green Chemistry, 23 (3), 1300–1311.

Kadhom, M. & Abdullah, G., 2016. Studying of two choline chloride's deep eutectic solvents in their aqueous mixtures. International Journal of Engineering Research and Development, 12, 73-80.

Kamlet, M. J. & Taft, R. W., 1976a. The solvatochromic comparison method. I. The .beta.-scale of solvent hydrogen-bond acceptor (HBA) basicities. Journal of the American Chemical Society, 98 (2), 377–383.

Kamlet, M. J., & Taft, R. W., 1976b. The solvatochromic comparison method. 2. The .alpha.-scale of solvent hydrogen-bond donor (HBD) acidities. Journal of the American Chemical Society, 98 (10), 2886-2894

Kamlet, M. J., Abboud, J. L. M., Abraham, M. H., and Taft, R. W., 1983. Linear solvation energy relationships. 23. A comprehensive collection of the solvatochromic parameters, .pi.*, .alpha., and .beta., and some methods for simplifying the generalized solvatochromic equation. The Journal of Organic Chemistry, 48 (17), 2877–2887.

Kamlet, M. J., Abboud, J. L. M., and Taft, R. W., 1981. An Examination of Linear Solvation Energy Relationships. Progress in Physical Organic Chemistry, 13, 485–630.

Kamlet, M. J., Abboud, J. L., and Taft, R. W., 1977. The solvatochromic comparison method. 6. The .pi.* scale of solvent polarities. Journal of the American Chemical Society, 99 (18), 6027–6038.

Klemm, D., Heublein, B., Fink, H.-P., and Bohn, A., 2005. Cellulose: Fascinating Biopolymer and Sustainable Raw Material. Angewandte Chemie International Edition, 44 (22), 3358–3393.

Klemm, D., Kramer, F., Moritz, S., Lindström, T., Ankerfors, M., Gray, D., and Dorris, A., 2011. Nanocelluloses: A New Family of Nature-Based Materials. Angew. Chem. Int. Ed., 50 (24), 5438–5466.

Klemm, D., Cranston, E. D., Fischer, D., Gama, M., Kedzior, S. A., Kralisch, D., Kramer, F., Kondo, T., Lindström, T., Nietzsche, S., Petzold-Welcke, K. and Rauchfuß, F., 2018. Nanocellulose as a natural source for groundbreaking applications in materials science: Today's state. Materials Today, 21 (7), 720–748.

Kondo, T., 1997. The relationship between intramolecular hydrogen bonds and certain physical properties of regioselectively substituted cellulose derivatives. journal of Polymer Science Part B: Polymer Physics, 35 (4), 717–723.

Lapeña, D., Errazquin, D., Lomba, L., Lafuente C. & Giner, B., 2021. Ecotoxicity and biodegradability of pure and aqueous mixtures of deep eutectic solvents: glyceline, ethaline, and reline. Environmental Science and Pollution Research, 28, 8812–8821

Laurence, C., Legros, J., Nicolet, P., Vuluga, D., Chantzis, A. & Jacquemin, D., 2014. Solvatomagnetic Comparison Method: A Proper Quantification of Solvent Hydrogen-Bond Basicity. The Journal of Physical Chemistry B, 118 (27), 7594-7608.

Laurence, C., Nicolet, P., Dalati, M. T., Abboud, J.-L. M., and Notario, R., 1994. The Empirical Treatment of Solvent-Solute Interactions: 15 Years of .pi.*. he Journal of Physical Chemistry, 98 (23), 5807–5816.

Laurence, C., Sergui, M., Daniela, V. & Julien, L., 2021. Measurement of the hydrogen bond acceptance of ionic liquids and green solvents by the 19F solvatomagnetic comparison method. Green Chemistry, 23 (4), 1816-1822.

Li, P., Sirviö, J. A., Haapala, A., and Liimatainen, H., 2017. Cellulose Nanofibrils from Nonderivatizing Urea-Based Deep Eutectic Solvent Pretreatments, ACS Appl. Mater. Interfaces, 9 (3), 2846–2855.

Longo Jr., L. S. and Craveiro, M. V., 2018. Deep Eutectic Solvents as Unconventional Media for Multicomponent Reactions. Journal of Brazilian Chemical Society, 29, 1999–2025.

Ma, Y., Xia, Q., Liu, Y., Chen, W., Liu, S., Wang, Q., Liu, Y., Li, J., and Yu, H., 2019. Production of Nanocellulose Using Hydrated Deep Eutectic Solvent Combined with Ultrasonic Treatment. ACS Omega, 4 (5), 8539–8547.

Madeira, P. P., Passos, H., Gomes, J., Coutinho, J. A. P., and Freire, M. G., 2017. Alternative probe for the determination of the hydrogen-bond acidity of ionic liquids and their aqueous solutions. Physical Chemistry Chemical Physics, 19 (18), 11011–11016.

Mannu, A., Blangetti, M., Baldino, S., and Cristina, P., 2021. Promising Technological and Industrial Applications of Deep Eutectic Systems, 14, 2494.

Marcus, Y., 1991. The effectiveness of solvents as hydrogen bond donors. Journal of Solution Chemistry, 20 (9), 929–944.

Meng, X., Ballerat-Busserolles, K., Husson, P., and Andanson, J.-M., 2016. Impact of water on the melting temperature of urea + choline chloride deep eutectic solvent. New Journal of Chemistry, 40 (5), 4492–4499.

Mjalli, F. S. and Ahmed, O. U., 2016. Physical properties and intermolecular interaction of eutectic solvents binary mixtures: reline and ethaline. Asia-Pasific Journal of Chemical Engineering, 11 (4), 549–557.

Moore, J. S., Prat-Resina, X., Wendorff, T., John W., & Hahn, A., 2020. Amphiprotic Species. Chemistry LibreTexts. [online] Retrieved: September 22, 2021, from https://chem.libretexts.org/@go/page/49517

Morais, E. S., Mendonça, P. V., Coelho, J. F. J., Freire, M. G., Freire, C. S. R., Coutinho, J. A. P., and Silvestre, A. J. D., 2018. Deep Eutectic Solvent aqueous solutions as efficient media for the solubilization of hardwood xylans. ChemSusChem, 11 (4), 753–762.

Muller, P., 1994. Glossary of terms used in physical organic chemistry (IUPAC Recommendations 1994). Pure and Applied Chemistry, 66 (5), 1077-1184.

Nechyporchuk O., Belgacem M.N., Bras J., 2016. Nanocellulose: production, functionalisation and applications. Industrial Crops and Products, 93, 2-25.

Oh, S. Y., Yoo, D. I., Shin, Y., and Seo, G., 2005. FTIR analysis of cellulose treated with sodium hydroxide and carbon dioxide. Carbohydrate Research, 340 (3), 417–428.

Palme, A., Theliander, H., and Brelid, H., 2016. Acid hydrolysis of cellulosic fibres: Comparison of bleached kraft pulp, dissolving pulps and cotton textile cellulose. Carbohydrate Polymers, 136, 1281–1287.

Proniewicz, L., Paluszkiewicza, C., Weseøucha-Birczynska, A., Majcherczykb, H., Baranski., A. & Konieczna, A., 2001. FT-IR and FT-Raman study of hydrothermally degradated. Journal of Molecular Structure, 596, 163-169.

Rani, M. A. A., Brant, A., Crowhurst, L., Dolan, A., Lui, M., Hassan, N. H., Hallett, J. P., Hunt, P. A., Niedermeyer, H., Perez-Arlandis, J. M., Schrems, M., Welton, T., and Wilding, R., 2011. Understanding the polarity of ionic liquids. Physical Chemistry Chemical Physics, 13 (37), 16831–16840.

Ray, A., Das, S., and Chattopadhyay, N., 2019. Aggregation of Nile Red in Water: Prevention through Encapsulation in β-Cyclodextrin. ACS Omega, 4 (1), 15–24.

Reichardt, C., 1965. Empirical Parameters of the Polarity of Solvents. Angewandte Chemie International Edition in English, 4 (1), 29–40.

Reichardt, C., 2005. Polarity of ionic liquids determined empirically by means of solvatochromic pyridinium N-phenolate betaine dyes. Green Chemistry, 7 (5), 339–351.

Reichardt, C., Welton, T., 2010. Solvent Effects on the Absorption Spectra of Organic Compounds. In Solvents and Solvent Effects in Organic Chemistry (eds C. Reichardt and T. Welton)., 7 (5), 339–351.

Röhrling, J., Potthast, A., Rosenau, T., Lange, T., Borgards, A., Sixta, H. & Kosma, P., 2002. A Novel Method for the Determination of Carbonyl Groups in Cellulosics by Fluorescence Labeling. 2. Validation and Applications. Biomacromolecules 3 (5), 969-975.

Saito, T. and Isogai, A., 2005. Ion-exchange behavior of carboxylate groups in fibrous cellulose oxidized by the TEMPO-mediated system. Carbohydrate Polymers, 61 (2), 183–190.

Saito, T., Nishiyama, Y., Putaux, J.-L., Vignon, M., and Isogai, A., 2006. Homogeneous Suspensions of Individualized Microfibrils from TEMPO-Catalyzed Oxidation of Native Cellulose. Biomacromolecules, 7 (6), 1687–1691.

Schneider, H., Badrieh, Y., Migron, Y., & Marcus, Y., 1992. Hydrogen Bond Donation Properties of Organic Solvents and Their Aqueous Mixtures from13C NMR Data of Pyridine-N-Oxide. Zeitschrift Für Physikalische Chemie, 177(Part 2), 143–156.

Schwanninger, M., Rodrigues, J. C., Pereira, H., and Hinterstoisser, B., 2004. Effects of short-time vibratory ball milling on the shape of FT-IR spectra of wood and cellulose. Vibrational Spectroscopy, 36 (1), 23–40.

Scopus database, 2021. Analyse results of documents by year “Deep eutectic solvent”. [online] Elsevier B.V. Available from: https://www.scopus.com/search/form.uri?zone=TopNavBar&origin=resultslist&display=basic#basic [Accessed 19.10.2021]

Selkälä, T., Sirviö, J. A., Lorite, G. S., and Liimatainen, H., 2016. Anionically Stabilized Cellulose Nanofibrils through Succinylation Pretreatment in Urea–Lithium Chloride Deep Eutectic Solvent. ChemSusChem, 9 (21), 3074–3083.

Singh, B. S., Lobo, H. R., and Shankarling, G. S., 2012. Choline chloride based eutectic solvents: Magical catalytic system for carbon–carbon bond formation in the rapid synthesis of β-hydroxy functionalized derivatives. Catalysis Communications, 24, 70–74.

Sirviö J.A., Hyypiö K., Asaadu S., Junka K. & Liimatainen H., 2020. High-strength cellulose nanofibers produced via swelling pretreatment based on a choline chloride–imidazole deep eutectic solvent. Green Chem, 22 (5), p.1763-1775.

Sirviö, J. A., Visanko, M., and Liimatainen, H., 2015. Deep eutectic solvent system based on choline chloride-urea as a pre-treatment for nanofibrillation of wood cellulose, Green Chem., 17 (6), 3401–3406.

Skulcova, A., Russ., A., Jablonsky., M. & Sima, J., 2018. The pH Behavior of Seventeen Deep Eutectic Solvents. BioResources, 13 (3), 5041-5051.

Swain, J. and Mishra, A. K., 2016. Nile red fluorescence for quantitative monitoring of micropolarity and microviscosity of pluronic F127 in aqueous media. Photochemical & Photobiological Sciences, 15 (11), 1400–1407.

Tang, X., Zuo, M., Li, Z., Liu (Sirviö et al. 2015, pp. 3401–3406), H., Xiong, C., Zeng, X., Sun, Y., Hu, L., Liu, S., Lei, T., and Lin, L., 2017. Green Processing of Lignocellulosic Biomass and Its Derivatives in Deep Eutectic Solvents. ChemSusChem. 10 (13), 2696-2706.

Teles, A., Capela, E., Carmo, J., Coutinho, J., Silvestere A. & Freire, M., 2017. Solvatochromic parameters of deep eutectic solvents formed by ammonium-based salts and carboxylic acids. Fluid Phase Equilibria, 448 (25), 15-21.

Tenhunen, T-M., Lewandowska, A., Orelma, H., Johansson, L-S., Virtanen, T., Harlin, A., Österberg, M., Eichhorn, S & Tammelin, T., 2018. Understanding the interactions of cellulose fibres and deep eutectic solvent of choline chloride and urea. Cellulose 25, 137–150.

Tomé, L. I. N., Baião, V., da Silva, W., and Brett, C. M. A., 2018. Deep eutectic solvents for the production and application of new materials. Applied materials today, 10, 30–50.

Wen, Q., Chen, J.-X., Tang, Y.-L., Wang, J., and Yang, Z., 2015. Assessing the toxicity and biodegradability of deep eutectic solvents. Chemosphere, 132, 63–69.

Xia, Q., Liu, Y., Meng, J., Cheng, W., Chen, W., Liu, S., Liu, Y., Li, J., and Yu, H., 2018. Multiple hydrogen bond coordination in three-constituent deep eutectic solvents enhances lignin fractionation from biomass. Green Chemistry, 20 (12), 2711–2721.

Xie, Y., Dong, H., Zhang, S., Lu, X., and Ji, X., 2014. Effect of Water on the Density, Viscosity, and CO2 Solubility in Choline Chloride/Urea. Journal of Chemical & Engineering Data, 59 (11), 3344–3352.

Xu, H., Peng, J., Kong, Y., Liu, Y., Su, Z., Li, B., Song, X., Liu, S., and Tian, W., 2020. Key process parameters for deep eutectic solvents pretreatment of lignocellulosic biomass materials: A review. Bioresource Technology, 310, 123416.

Xue, Z., Zhao, X., Sun, R., and Mu, T., 2016. Biomass-Derived γ-Valerolactone-Based Solvent Systems for Highly Efficient Dissolution of Various Lignins: Dissolution Behavior and Mechanism Study. ACS Sustainable Chemistry Engineering, 4 (7), 3864–3870.

Yu, W., Wang, C., Yi, Y., Wang, H., Zeng, L., Li, M., Yang, Y. and Tan, Z., 2020. Comparison of Deep Eutectic Solvents on Pretreatment of Raw Ramie Fibers for Cellulose Nanofibril Production. ACS Omega, 5 (10), 5580–5588.

Zdanowicz, M., Wilpiszewska, K., and Spychaj, T., 2018. Deep eutectic solvents for polysaccharides processing. A review. Carbohydrate Polymers, 200, 361–380.

Zhang, H., Lang, J., Lan, P., Yang, H., Lu, J., & Wang, Z., 2020. Study on the Dissolution Mechanism of Cellulose by ChCl-Based Deep Eutectic Solvents. Materials (Basel, Switzerland), 13 (2), 278.

Zhang, Q., Vigier, K. D. O., Royer, S., and Jérôme, F., 2012. Deep eutectic solvents: syntheses, properties and applications. Chemical Society Reviews, 41 (21), 7108–7146.

Zhang, Y., Yin, C., Zhang, Y., & Wu, H., 2013. Synthesis and characterization of cellulose carbamate from wood pulp, assisted by supercritical carbon dioxide. BioResources, 8(1), 1398-1408.

Zhao, D., Liao, Y., and Zhang, Z., 2007. Toxicity of Ionic Liquids. CLEAN -Soil, Air, Water., 35 (1), 42–48.

Zhekenov, T., Toksanbayev, N., Kazakbayeva, Z., Shah, D. & Mjalli, F., 2017. Formation of type III Deep Eutectic Solvents and effect of water on their intermolecular interactions. Fluid Phase Equilibria, 441, 43-48.

Zhu, Y., Wu, C., Yu, D., Ding, Q. & Li, R., 2021. Tunable micro-structure of dissolving pulp-based cellulose nanofibrils with facile prehydrolysis process. Cellulose, 28, 3759–3773.

Znamenskiy ,V. & Kobrak, M. N., 2004. Molecular Dynamics Study of Polarity in Room-Temperature Ionic Liquids. The Journal of Physical Chemistry B, 108 (3), 1072-1079.

APPENDICES

Appendix 1. FS5 analysis, all particles.

Appendix 2. Wavelengths corresponding to maximum absorption of the probes 4-nitroaniline (4NA), N,N-diethyl-4-nitroaniline (DENA) and Nile Red (NR).

Appendix 3. Viscosities of DESs with different shear rates in 20 °C and in 100 °C.

Appendix 1. FS5 analysis, all particles.

SP name	molar ratio (CC: U:water)	Lc(l) ISO [mm]	Fiber width [µm]	Curl [%]	Kink [1/m]	Kink angle [deg]
1:2:0	1:2:0	1.675	18.98	14.68	3489.1	30.63
1:2:2	1:2:2	1.673	19.44	14.65	3411.7	30.76
1:2:4	1:2:4	1.66	19.72	16.18	3613.7	31.75
1:2:6	1:2:6	1.678	20.17	15.48	3536.3	31
1:2:8	1:2:8	1.679	20.66	15.74	3570.3	31.25
1:2:10	1:2:1	1.681	20.35	15.34	3399.3	31.11
1:1:0	1:1:0	1.672	18.87	15.25	3551.2	31.16
1:1:2	1:1:2	1.695	20.25	15.56	3491	31.48
1:1:4	1:1:4	1.674	20.19	15.26	3529	31.53
1:1:6	1:1:6	1.667	20.64	16.02	3679.1	32.2
1:1:8	1:1:8	1.666	20.07	16.44	3629.7	32.56
1:1:10	1:1:10	1.677	20.7	15.43	3513	31.38
1:0.5:0	2:1:0	1.649	19.86	15.72	3330.8	32.08
1:0.5:2	2:1:2	1.687	20.28	15.2	3497.1	31.29
1:0.5:4	2:1:4	1.658	20.09	15.92	3511.1	32.06
1:0.5:6	2:1:6	1.681	20.1	14.73	3355.1	30.89
1:0.5:8	2:1:8	1.672	20.14	14.96	3353.9	31.2
1:0.5:10	2:1:10	1.677	19.81	16.35	3557.8	32.01
REF CC	1:0:2	1.865	20.11	15.92	4043.1	31.62
REF Urea	0:1:2	1.676	20.7	15.4	3339.7	30.2
REF Water	0:0:2	1.851	18.9	16.01	3883.6	30.61
havuREF	0:0:2	1.644	18.62	14.58	3467	31.11
REFwater NaOH	0:0:2	1.6	19.71	18.01	3804.2	33.77
refCCNaOH	0:1:2	1.67	20.33	15.28	3502.8	31.46

Appendix 2. Wavelengths corresponding to maximum absorption of the probes 4-nitroaniline (4NA), N,N-diethyl-4-nitroaniline (DENA) and Nile Red (NR).

Sample	4NA (nm)	DENA (nm)	NR (nm)
1:2:0	389	422	567
1:2:2	388	425	575
1:2:4	387	422	581
1:2:6	384	428	585
1:2:8	387	429	586
1:2:10	387	428	588
1:1:2	387	423	573
1:1:4	388	427	577
1:1:6	385	427	584
1:1:8	390	427	585
1:1:10	385	428	590
1:0.5:2	388	422	570
1:0.5:4	387	423	580
1:0.5:6	386	426	583
1:0.5:8	386	426	585
1:0.5:10	384	428	587
refCC	390	422	569
refWater	381	429	590*
CycloHex	323	361	490
DMSO	391	412	577

*= peak is determined with peak fitting software

Appendix 3. Viscosities of DESs with different shear rates in 20 °C and in 100 °C.

Sample name	Viscosity at 20 °C Pa.s 0.1/s	Viscosity at 20 °C Pa.s 10/s	Viscosity at 100 °C Pa.s 0.1/s	Viscosity at 100 °C Pa.s 0.25/s	Viscosity at 100 °C Pa.s 10/s
1:2:0	-	-	73.00	36.54	0.21
1:2:2	87.34	1.31	3.98	12.80	0.14
1:2:4	111.57	1.16	0.59	2.75	0.16
1:2:2	104.78	1.30	16.44	16.83	0.13
1:2:8	101.69	1.42	0.37	0.33	0.15
1:2:10	103.86	1.52	46.50	28.67	0.22
1:1:0	-	-	56.78	26.44	0.26
1:1:2	102.25	1.44	1.99	12.63	0.17
1:1:4	135.51	1.41	12.90	15.59	0.21
1:1:6	84.14	1.18	9.36	9.78	0.18
1:1:8	106.90	1.56	29.68	18.17	0.19
1:1:10	99.52	1.39	45.71	25.22	0.29
1:0.5:0	-	-		-	-
1:0.5:2	100.16	1.43	0.33	11.93	0.37
1:0.5:4	116.14	1.36	51.75	30.73	0.24
1:0.5:6	94.16	1.53	5.19	9.37	0.29
1:0.5:8	101.22	1.42	30.45	18.50	0.15
1:0.5:10	113.54	1.71	19.47	13.86	0.20
refCC	102.10	1.42	304.14	288.64	0.77
refUrea	-	-	78.97	31.78	0.20